Factors controlling the community structure of picoplankton in contrasting marine environments

Jose Luis Otero-Ferrer[1], Pedro Cermeño[2], Antonio Bode[6], Bieito Fernández-Castro[1,3], Josep M. Gasol[2,5], Xosé Anxelu G. Morán[4], Emilio Marañon[1], Víctor Moreira-Coello[1], Marta M. Varela[6], Marina Villamaña[1], and Beatriz Mouriño-Carballido[1]

[1]Departamento de Ecoloxía e Bioloxía Animal, Universidade de Vigo, Spain
[2]Institut de Ciències del Mar, Consejo Superior de Investigaciones Científicas-Barcelona, Spain
[3]Departamento de Oceanografía, Instituto de investigacións Mariñas (IIM-CSIC), Vigo, Spain
[4]King Abdullah University of Science and Technology (KAUST), Read Sea Research Center, Biological and Environmental Sciences and Engineering Division, Thuwal, Saudi Arabia.
[5]Centre for Marine Ecosystem Research, School of Sciences, Edith Cowan University, WA, Australia
[6]Centro Oceanográfico de A Coruña, Instituto Español de Oceanografía, A Coruña, Spain.

Correspondence to: Jose Luis Otero-Ferrer (jootero@uvigo.es)

Abstract. The effect of inorganic nutrients on planktonic assemblages has been traditionally relied on concentrations rather than estimates of nutrient supply. We combined a novel dataset of hydrographic properties, turbulent mixing, nutrient concentration and picoplankton community composition with the aim of: i) quantifying the role of temperature, light and nitrate fluxes as factors controlling the distribution of autotrophic and heterotrophic picoplankton subgroups, as determined by flow cytometry; and ii) describing the ecological niches of the various components of the picoplankton community. Data were collected in 97 stations in the Atlantic Ocean, including tropical and subtropical open ocean waters, the northwestern Mediterranean Sea, and the Galician coastal upwelling system of the Northwest Iberian Peninsula. A Generalized Additive Model (GAM) approach was used to predict depth-integrated biomass of each picoplankton subgroup based on three niche predictors: sea surface temperature, averaged daily surface irradiance, and the transport of nitrate into the euphotic zone, through both diffusion and advection. In addition, niche overlap between different picoplankton subgroups was computed using non-parametric kernel density functions. Temperature and nitrate supply were more relevant than light in predicting the biomass of most picoplankton subgroups, except for *Prochlorococcus* and low nucleic acid (LNA) prokaryotes, for which irradiance also played a significant role. Nitrate supply was the only factor that allowed the distinction between the ecological niches of all autotrophic and heterotrophic picoplankton subgroups. *Prochlorococcus* and LNA prokaryotes were more abundant in warmer waters (> 20ºC) where the nitrate fluxes were low, whereas *Synechococcus* and high nucleic acid (HNA) prokaryotes prevailed mainly in cooler environments characterized by intermediate or high levels of nitrate supply. Finally, the niche of picoeukaryotes was defined by low temperatures and high nitrate supply. These results support the key role of nitrate supply, as it not only promotes the growth of large phytoplankton, but it also controls the structure of marine picoplankton communities.

1 Introduction

Picoplankton, including archaea, bacteria and picoeukaryotes are the smallest (cell diameter <2 μm) and most abundant organisms in marine ecosystems. Photosynthetic picoplankton often dominate marine phytoplankton biomass and primary production in oligotrophic tropical and subtropical regions (Chisholm, 1992), whereas they are typically a minor component in nutrient-replete coastal environments, usually dominated by large-sized plankton species (Finkel et al., 2010; Marañón, 2015). However, due to the large temporal and spatial variability in the structure and composition of the microbial community in shelf seas (Sherr et al., 2005), picoplankton, together with nanoplankton, can dominate the microbial community under certain conditions (Morán, 2007; Espinoza-González et al., 2012). In addition, picoplankton contributes overwhelmingly to the recycling of organic matter (Azam et al., 1983; Fenchel, 2008), and previous studies suggest that photosynthetic picoplankton could also play a role in the export of carbon to the deep ocean (Richardson and Jackson, 2007; Lomas and Moran, 2011; Guidi et al., 2015). As a result, picoplankton is considered a key component of the current carbon cycle and likely more important in future climate warming scenarios (Laufkötter et al., 2016).

When analyzed by flow cytometric techniques, two genera of picocyanobacteria (*Prochlorococcus* and *Synechococcus*), one or two subgroups of autotrophic picoeukaryotes of different size (small and large), and two subgroups of heterotrophic prokaryotes, based on their high (HNA) or low nucleic acid (LNA) content, can be distinguished (Gasol and del Giorgio, 2000; Marie and Partensky, 2006). Although closely related phylogenetically, *Synechococcus* and *Prochlorococcus* exhibit distinct physiological traits (Moore et al., 1995), divergent evolutionary strategies (Scanlan and West, 2002) and disparate geographic distributions (Zubkov et al., 2000). *Prochlorococcus* tend to be restricted to relatively warm (above 15ºC) and nutrient-poor waters, extending from the surface down to 150 m, along the 40º N–40º S latitudinal band (Partensky et al., 1999b; Johnson et al., 2006). *Synechococcus* exhibit a wider geographic and thermal distribution, including high-nutrient waters and occasionally reaching polar latitudes (Paulsen et al., 2016), their vertical distribution being shallower than that of *Prochlorococcus* (Partensky et al., 1999a; Li, 2002). The contribution of picoeukaryotes to picoplankton biomass is generally smaller than the contribution of picocyanobacteria (Zubkov et al., 2000; Buitenhuis et al., 2012), except in coastal regions where their contribution usually increases (Grob et al., 2007). In general, LNA prokaryotes dominate heterotrophic prokaryotic biomass in the oligotrophic open ocean, whereas HNA cells dominate in coastal regions (Li et al., 1995; Bouvier et al., 2007). These contrasting spatial distributions suggest that the picoplankton subgroups occupy differential ecological niches or, according to the classical definition proposed by Hutchinson (1957), distinct multidimensional hypervolumes of environmental factors in which viable populations develop. By describing the overlaps of environmental factors, realized niche partitioning can be defined, and the factors controlling the distribution of picoplankton subgroups can be identified. However, despite decades of experimental and field observations, the relative importance of the factors driving the variability of the growth and the spatial distribution of picoplankton subgroups remain largely unknown.

Aside from the effect of trophic controls, the distribution of microbial plankton is primarily determined by seawater temperature, light and nutrients (Li, 2009, 2007; Barton et al., 2015). Quantifying their relative influence on the spatial and temporal distribution of the different picoplankton subgroups is complicated by the fact that the above mentioned factors are often

correlated in the ocean (Finkel et al., 2010). This shortcoming can be circumvented by using experimental approaches in the laboratory, where the influence of each independent factor is isolated. Alternatively, it can be approached by combining large data sets of hydrographic and biological observations collected from contrasting marine environments, which allow to characterize the suite of variables that best define the organism's ecological niches.

5   In order to study the significance of temperature and nutrient concentrations in determining the contribution of picophytoplankton to total phytoplankton biomass and production, Agawin et al. (2000) reviewed the available literature from oceanic and coastal estuarine areas. Although the number of observations for which both temperature and nutrient concentration were available was too small to statistically separate their effects, these authors hypothesized that the dominance of picoplankton in warm, oligotrophic waters was due to differences between picophytoplankton and larger cells in the capacity to use nutri-

10   ents and in their intrinsic growth rate. Bouman et al. (2011) investigated how vertical stratification controls the community structure of picophytoplankton in subtropical regions. According to their results, photosynthetic picoeukaryotes dominate in weakly-stratified, whereas in strongly stratified waters, *Prochlorococcus* cyanobacteria are prevalent. More recently, Flombaum et al. (2013), using a compilation of flow cytometry data from all major ocean regions, concluded that *Prochlorococcus* and *Synechococcus* abundance distributions were controlled by temperature and photosynthetically active radiation (PAR, 400-700

15   nm), discarding the role of nitrate concentration. However, in tropical and subtropical domains, the best represented regions in Flombaum et al.'s study, surface nitrate is almost depleted and the variability of its concentration can be widely disconnected from changes in its availability for phytoplankton, which depends more on the supply from deeper waters by turbulent diffusion (Mouriño-Carballido et al., 2016). It is also believed that fine-scale turbulence can enhance the nutrient uptake and subsequent growth of larger phytoplankton (Lazier and Mann, 1989; Karp-Boss et al., 1996; Guasto et al., 2012), especially in regions

20   with low nutrient levels and strong grazing pressure (Barton et al., 2014).

As far as we know, only one study has previously used estimates of nitrate availability, derived from observations of microstructure turbulence, to investigate the role of nutrient availability in controlling the composition of picoplankton communities (Mouriño-Carballido et al., 2016). These authors, using local data from the northwestern Mediterranean Sea, found that different autotrophic picophytoplankton subgroups exhibit contrasting responses to nitrate supply, and that as a result the

25   ratio of prokaryotic to picoeukaryotic photoautotrophic biomass decreased with increasing nitrate supply. However, whether these patterns are general and widespread in the ocean remains largely uncertain, given that no concomitant datasets including measurements of turbulent diffusion nutrient flux and picoplankton subgroup structure have been available to date.

Here we extend the analysis described in Mouriño-Carballido et al. (2016) by combining a dataset of picoplankton community composition, hydrographic properties, turbulent mixing and inorganic nutrient concentrations collected in a total of 97

30   stations. Observations were made in contrasting environments of the Atlantic Ocean, in order to quantify the role of temperature, light and nitrate availability in the composition of the picoplankton community, and to describe the ecological niches of each picoplankton subgroup.

2   Material and Methods

This study includes data collected in 97 stations from three contrasting environments covering the tropical and subtropical Atlantic Ocean (T), the northwestern Mediterranean Sea (M), and the Galician coastal upwelling ecosystem (G), between October 2006 and December 2015 (Table 1 and Figure 1). Two cruises (CARPOS Oct-Nov 2006 and TRYNITROP Apr-May 2008) sampled 26 stations located in the tropical and subtropical Atlantic Ocean. Three other cruises carried out in the Mediterranean Sea (FAMOSO1 Mar 2009, FAMOSO2 Apr-May 2009, and FAMOSO3 Sep 2009) sampled 19 stations during three contrasting hydrographic conditions, covering from winter mixing to summer stratification. Finally, 52 stations were sampled in the Galician coastal upwelling ecosystem during HERCULES1 Jul 2010, HERCULES2 Sep 2011, HERCULES3 Jul 2012, DISTRAL Feb-Nov 2012, ASIMUTH Jun 2013, CHAOS Aug 2013, and NICANOR Feb 2014-Dec 2015 cruises. Additional information about the sampling design of these cruises is presented in Aranguren-Gassis et al. (2011, CARPOS), Mouriño-Carballido et al. (2011, TRYNITROP), Mouriño-Carballido et al. (2016, FAMOSO), Cermeño et al. (2016, DISTRAL), Villamaña et al. (2017, CHAOS) and Moreira-Coello et al. (2017, NICANOR).

At each station, information about hydrographic properties, turbulent mixing, nitrate concentration and picoplankton community composition were collected. Light conditions for each sampling station were considered as the 5-day averaged daily surface photosynthetic active radiation (PAR) obtained from satellite data (http://globcolour.info). Light attenuation coefficients were obtained from vertical profiles of PAR estimated by Licor sensors using the Beer-Lambert Law equation (Kirk, 1994). Depth of the euphotic layer was calculated as the depth where PAR was 1% of its surface value. For those cruises where PAR profiles were not available (ASIMUTH, CHAOS and NICANOR), which sampled stations in the outer part of the Galician Rías, the depth of the photic layer was calculated by considering light attenuation coefficients derived from surface chlorophyll-a data, following the algorithms proposed by Morel et al. (2007) for Case-1 waters ($log_{10}Z_{eu} = 1.524 - 0.460[Chl]_{surf} - 0.00051[Chl]_{surf}^2 + 0.0282[Chl]_{surf}^3$). A comparison of the estimation of the base of the euphotic zone by using the Morel et al. (2007) equation and the data collected by a radiometer during the HERCULES cruise is shown in Figure A1-A.

2.1   Hydrography and turbulent mixing

Hydrographic properties and turbulent mixing were derived from a microstructure turbulent profiler (Prandke and Stips, 1998, MSS) equipped with a high-precision Conductivity-Temperature-Depth (CTD) probe, two microstructure shear sensors (type PNS06), and also a sensor to measure the horizontal acceleration of the profiler. Measurements of dissipation rates of turbulent kinetic energy (ε) were conducted to the bottom, or to 137-323 m over deep waters (Table 1). The number of microstructure turbulence profiles used for computing nitrate fluxes at each station were always deployed successively. Sets include 2-11 in the tropical and subtropical Atlantic (37 ± 18 min), 6-7 in the Mediterranean (76 ± 22 min) and 3-402 in the Galician coastal upwelling (65 ± 246 min) (Figure A1-B). Episodic bursts of turbulence can induce episodic inputs of nutrient supply which can be easily missed in sets of low number of profiles. In coastal regions where short-term variability of mixing processes is expected to be higher, our dataset includes two high-frequency samplings carried out in the outer part of Ría de Vigo (Galician

upwelling ecosystem) in August 2013 (CHAOS cruises). During these cruises two 25-hour series of turbulent microstructure and currents observations were carried out during spring and neap tides. Turbulent kinetic energy dissipation at the interface between upwelled and surface waters was enhanced by two orders of magnitude during the ebbs, as the result of the interplay of the bi-directional upwelling circulation and the tidal currents shear (Fernández-Castro et al., 2018). Diffusive nitrate fluxes due to the enhanced dissipation observed during spring tide, could be responsible for about half of the phytoplankton primary production estimated in this system during periods of upwelling relaxation-stratification (Villamaña et al., 2017).

The profiler was balanced to have negative buoyancy and a sinking velocity of 0.4 to 0.7 m s^{-1}. The frequency of data sampling was 1024 Hz. The sensitivity of the shear sensors was checked after each use. Due to significant turbulence generation close to the ship, only the data below 5 (HERCULES1, HERCULES2, HERCULES3, DISTRAL, ASIMUTH, CHAOS, and NICANOR) and 10 m (CARPOS, TRYNITROP, FAMOSO1, FAMOSO2, FAMOSO3) were considered reliable. Data processing and calculation of dissipation rates of (ε) was carried out with the commercial software MSSpro. The squared Brunt Väisälä frequency (N^2) was computed from the CTD profiles according to the equation:

$$N^2 = -\left(\frac{g}{\rho_w}\right)\left(\frac{\partial \rho}{\partial z}\right)(s^{-2}) \tag{1}$$

where g is the acceleration due to gravity (9.8 m s^{-2}), ρ_w is seawater density (1025 kg m^{-3}), and $\partial\rho/\partial z$ is the vertical potential density gradient. Vertical diffusivity (K_z) was estimated as:

$$K_z = \Gamma\frac{\varepsilon}{N^2}(m^2 s^{-1}) \tag{2}$$

where Γ is the mixing efficiency, here considered as 0.2 (Osborn, 1980).

2.2 Nutrient supply

Samples for the determination of nitrate (NO$_3$) + nitrite (NO$_2$) were collected from 5±2 (Galician coastal upwelling), 7±1 (Mediterranean) and 11±2 (tropical and subtropical Atlantic Ocean) depths in rinsed polyethylene tubes and stored frozen at -20 °C until analysis on land, according to standard methods using the automated colorimetric technique (Grasshoff et al., 2007). The frequency histogram of sampling depths collected for nitrate concentration in each region is indicated in Figure A1-C, whereas the maximum sampling depth where the microstructure turbulence profiler was deployed is indicated in Table 1. In one station carried out during the NICANOR cruises, where nitrate concentrations were not available, these were obtained by using a nitrate-density relationship built by using all samples (n=52) collected during the NICANOR sampling period. The relationship showed a linear behavior ($NO_3 = 9.7788 * \sigma_t - 256.38$; Adj-r^2=0.87; p < 0.001) for density ranging between 26.1 and 27.1 kg m^{-3} (Figure A1-D).

Vertical diffusive fluxes of nitrate into the euphotic zone were calculated following the Fick's law as:

$$FluxNO_3 = \bar{K}_z\Delta NO_3 \tag{3}$$

where ΔNO_3 is the nitrate vertical gradient obtained by linear fitting of nitrate concentrations in the nitracline, determined as a region of approximately maximum and constant gradient, and ($\bar{K}_z$) is the averaged turbulent mixing over the same depth

interval. In the Galician coastal upwelling, nitrate diffusive fluxes were estimated over a fixed depth interval using the same procedure (20-40 m) except in the shallowest stations where we compute the surface-bottom flux.

Most stations carried out in the Galician coastal upwelling were conducted inside three different Rías (Ría de Vigo, Ría de Pontevedra and Ría de A Coruña). The Rías are coastal embayments affected by seasonal wind-driven coastal upwelling of cold, nutrient-rich North Atlantic Central water (Wooster et al., 1976; Fraga, 1981; Álvarez-Salgado et al., 1993). The Galician Rías, despite being in general longer and narrower than many open bays in upwelling areas, they resemble them in that its primary hydrographic and circulation features are determined by the extension of wind-driven flow on the external continental shelf throughout the bay (Alvarez-Salgado et al., 2010). Fertilization in the Rías occurs essentially by coastal upwelling, being fresh and rain water inputs residual (2%) (Fernández et al., 2016). The total nitrate supply in the Galician Rías was computed as the sum of nitrate vertical diffusion plus nitrate vertical advection due to coastal upwelling. A simplified estimate of nitrate supply through vertical advection due to upwelling was computed considering the Galician Rías as single boxes divided into two layers (Álvarez-Salgado et al., 1993), the deeper one influenced by upwelled inflowing waters and the surface layer dominated by the outgoing flow. Assuming that the bottom layer volume is conservative and stationary, the vertical advective flux (Q_Z, m^3s^{-1}), would be equivalent to the incoming bottom flux (Q_B, m^3s^{-1}), computed as the product of the upwelling index ($I_W, m^3s^{-1}km^{-1}$) and the lengths of the mouth of the Rías (ca. 10-11.5 km). I_W was averaged over the three-day period before each cruise from wind data recorded by meteorological buoys located in Cabo Vilano (HERCULES, NICANOR) and Cabo Silleiro (DISTRAL, ASIMUTH, CHAOS, ASIMUTH), or modeled by the Fleet Numerical Meteorology and Oceanography Center (FNMOC) model when buoy data were not available (http://www.indicedeafloramiento.ieo.es). Finally, the transport of nitrate into the euphotic zone through vertical advection was computed as:

$$NO_3 \, Advective \, flux = \frac{Q_z}{A_{basin}} [NO_3]_D \quad\quad\quad (4)$$

where A_{basin} is the surface area of the Galician Rías, Q_Z is the vertical advective flux, and $[NO_3]_D$ is the averaged nitrate concentration at the base of the euphotic layer. A_{basin} is 141 km^2 for Ría de Pontevedra (ASIMUTH), 174 km^2 for Ría de Vigo (CHAOS, ASIMUTH, DISTRAL), and 145 km^2 for Ría de A Coruña (HERCULES, NICANOR) (see Villamaña et al. 2017 and Moreira-Coello et al. 2017, for details).

2.3 Flow cytometry

Picoplankton samples (1.8 ml) for the determination of picoplankton abundance and cell properties were taken from 3-9 depths and measured immediately on board (TRYNITROP), or preserved with paraformaldehyde plus glutaraldehyde (P+G) and frozen at $-80°$ C until analysis in the laboratory (the other cruises). Unfortunately, due to problems with sample preservation, only heterotrophic or autotrophic picoplankton subgroup data were available for the DISTRAL and ASIMUTH cruises, respectively. Two aliquots from the same sample were used for the study of picophytoplankton (0.6 ml) and heterotrophic prokaryotes (0.4 ml), analyzed at high (mean 60 μl min^{-1}) and low (mean 18 μl min^{-1}) flow rates during 4 and 2 min, respectively. Before the analysis, the DNA of heterotrophic prokaryotes was stained with nucleic acid-specific fluorescent dye (SYTO-13 or SYBR1). A FACSCalibur flow cytometer (Becton-Dickinson) equipped with a laser emitting at 488 nm was

used to measure and count picoplankton. Autotrophic cells were separated into two groups of cyanobacteria (*Synechococcus* and *Prochlorococcus*) and one group of small picoeukaryotes, based on their fluorescence and light scatter signals (SSC), as explained in (Calvo-Díaz and Morán, 2006). Two groups of heterotrophic prokaryotes (LNA and HNA) were distinguished based on their relative green fluorescence, which was used as a proxy for nucleic acid content (Gasol and del Giorgio, 2000; Bouvier et al., 2007).

In order to estimate biovolume (BV), we used an empirical calibration between Size SCatter (SSC) and cell diameter (Calvo-Díaz and Morán, 2006), assuming spherical shape for all groups. The following volume-to-carbon conversion factors were used for picoautotrophic groups: 230 fg C BV for *Synechococcus*, 240 fg C BV for *Prochlorococcus* and 237 fg C BV for picoeukaryotes (Worden et al., 2004). For bacteria BV was converted into carbon biomass by using the allometric relationship: 108.8 fg C BV$^{0.898}$ (Gundersen et al., 2002). More details about the processing and analysis of flow cytometry samples are provided in Calvo-Díaz and Morán (2006, TRYNITROP), Gomes et al. (2015, FAMOSO), Villamaña et al. (2017, CHAOS) and Moreira-Coello et al. (2017, NICANOR). Abundance data obtained at different depths for each station were combined to compute depth-integrated biomass for the photic layer.

2.4 Generalized Additive Models

A Generalized Additive Model (GAM) approach was used to predict depth-integrated biomass of each picoplankton subgroup, the contribution of LNA prokaryotes to heterotrophic picoplankton, the cyanobacteria to picoeukaryotes ratio, and the autotrophic to heterotrophic ratio based on observations and estimates of three environmental factors: sea surface temperature (SST), daily surface PAR, and the transport of nitrate into the euphotic zone (NO$_3$ Flux), including both diffusive and advective processes. GAMs assume that the effect of each predictor on the response variable can be described by smoothed functions whose effects are additive. Due to the large number of zero observations, data overdispersion, and the need for a single parsimonious model to make predictions for a large number of groups, we assumed that the depth-integrated biomass of each picoplankton subgroup, relative contribution values and biomass ratios all followed negative binomial distributions. Those niche descriptors that did not follow normal distributions were log transformed. The complete model structure for the biomass of each picoplankton subgroup was:

$$y_j = I + s(SST) + s(PAR) + s(\log(NO_3 Flux)) + Error \tag{5}$$

where y_j represents the depth-integrated biomass for each picoplankton subgroup j, and s a cubic regression spline used for fitting the observations to the model (Wood, 2006).

Generalized models include a function linking the mean value of y_j and the predictors. For those response variables that followed a negative binomial distribution the used link function was the natural logarithm. The LNA contribution to total heterotrophic prokaryotes was adjusted using a gaussian distribution and an identify link (Wood et al., 2016). The inclusion of the different predictors to explain the response variable (the biomass of each picoplankton subgroup, its relative contribution and biomass ratios) was assessed via stepwise model selection using the minimum Akaike Information Criterion (Hastie and Tibshirani, 1993).

Smooth terms were tested using a Bayesian test (Marra and Wood, 2012) to prevent overfitting. GAMs were evaluated based on explanatory power (explained variance) and goodness-of-fit (GOF). GOF was assessed via quantile–quantile (QQ) plots of Pearson residuals (provided in SM Figure A2). All calculations were done using the mgcv package (Wood, 2011) in R (R Core Team, 2015).

2.5   Niche overlap analysis

The estimation of niche overlap between different picoplankton subgroups based on non-parametric kernel density functions (NO_K) was calculated following Mouillot et al. (2005):

$$NO_{K\,i,j,t} = 1 - \frac{1}{2} \int |f_{it}(x) - f_{jt}(x)|\, dx \tag{6}$$

where $NO_{K_{i,\,j,\,t}}$ is the niche overlap between picoplankton subgroups i and j for the environmental factor t, and f_{it} and f_{jt} are the kernel population density functions of factor t for species i and j, respectively. In order to correct the correlation between niche predictors, we used the estimator in a dependent sample (EDS) proposed by Kark et al. (2002).

To assess the statistical niche differences between subgroups, null model permutation tests were performed to verify whether the niche overlaps were significantly lower than 100% (Geange et al., 2011). When the contribution of depth-integrated biomass for each picoplankton subgroup exceeded that expected by chance ($1/3$ for autotrophic and $1/2$ for heterotrophic picoplankton), niche predictors for each station were selected. Statistical null distributions (the distribution of the statistic test under the null hypothesis of no niche differentiation) were generated by calculating pseudo-values through randomly permuting group labels in the corresponding data set over 10000 runs. The distributions of the average niche overlaps for the null model were then computed. Niche overlap calculations and associated null model tests were performed using the density function and the source code provided as supporting information in Geange et al. (2011). All calculations were done using R (R Core Team, 2015).

3   Results

3.1   Environmental variables and picoplankton biomass

Our database covered a wide environmental gradient from oligotrophic to eutrophic conditions. Stations sampled in the tropical and subtropical Atlantic oceans (T) were, on average, characterized by warm surface waters (26 ± 2 ℃, mean $\pm$ SD) where the supply of nitrate through vertical diffusion from deeper waters (0.7 ± 1.6 mmol N m^{-2} d^{-1}), and surface chlorophyll-a were low (0.1 ± 0.1 mg m^{-3}) (Table 2 and Figure 2). The Mediterranean Sea (M), sampled from March to September, was characterized by cooler surface waters (16 ± 4 ℃), and intermediate values of both nitrate vertical diffusive supply (41 ± 113 mmolN m^{-2} d^{-1}) and also surface chlorophyll-a (0.9 ± 0.9 mg m^{-3}). Finally, the stations sampled in the Galician coastal upwelling system (G), which included year-round samples, were characterized by relatively cold surface waters (16 ± 2 ℃), enhanced rates of nitrate supply (30 ± 46 mmolN m^{-2} d^{-1}) and high values of surface chlorophyll-a (2.2 ± 2.5 mg m^{-3}). No statistically significant differences were observed in averaged surface photosynthetic active radiation between the three regions.

Differences in picoplankton biomass and composition were also observed between the three domains. Averaged photic layer depth-integrated total picoplankton biomass (including both LNA and HNA prokaryotes, *Prochlorococcus*, *Synechococcus* and picoeukaryotes) was higher in the tropical and subtropical Atlantic (1052 ± 215 mg C m^{-2}) and the Mediterranean (1038 ± 485 mg C m^{-2}), compared to the Galician coastal upwelling (216 ± 36 mg C m^{-2}) (Table 2). In the tropical and subtropical Atlantic, the contribution of *Prochlorococcus* to total picoplankton biomass was 41%, followed by LNA (27%) and HNA (22%) prokaryotes, with smaller contributions of *Synechococcus* and picoeukaryotes (<5% each). In the Mediterranean, picoplankton biomass was on average dominated by *Synechococcus* (50%), followed by LNA and HNA prokaryotes ($\sim$17% for each group), picoeukaryotes (10%) and *Prochlorococcus* (5%). Finally, HNA (55%) and LNA (21%) prokaryotes dominated in the Galician coastal upwelling system, followed by picoeukaryotes (11%), *Synechococcus* (6%) and *Prochlorococcus* (1%).

Vertical distributions of temperature, nitrate concentration and the biomass of autotrophic and heterotrophic picoplankton groups for each domain are shown in Figure A3.

3.2 The role of environmental factors in picoplankton composition

In order to explore the role of temperature, light and nitrate supply in the composition of the picoplankton community, we first used Generalized Linear Models to investigate simple linear relationships between each of these factors and the depth-integrated biomass of each picoplankton subgroup, the contribution of LNA prokaryotes to heterotrophic picoplankton biomass, the cyanobacteria (*Prochlorococcus* and *Synechococcus*) to picoeukaryotes ratio, and the autotrophic to heterotrophic picoplankton ratio (Figure 3 and Table 3). All picoplankton groups except picoeukaryotes exhibited statistically significant relationships with sea surface temperature. This relationship was negative for *Synechococcus*, and positive for all the other subgroups (Figure 3). Only LNA and HNA prokaryotes and *Synechococcus* exhibited significant, positive relationships with surface radiation. All groups except the picoeukaryotes were negatively correlated with nitrate fluxes. The contribution of LNA prokaryotes to heterotrophic picoplankton biomass only exhibited a significant negative relationship with nitrate fluxes, whereas the cyanobacteria to picoeukaryotes ratio was positively correlated with surface temperature and negatively with nitrate fluxes. Finally, the ratio of autotrophic to heterotrophic biomass was not linearly correlated with any of the studied environmental factors. In order to exclude cross-correlation between the three environmental factors and consider the possibility of non-linear relationships, we subsequently fitted the data to Generalized Additive Models (Figure 4 and Table 3). Temperature was the only factor included in the models built for predicting the depth-integrated biomass of all picoplankton subgroups. HNA prokaryotes exhibited a positive relationship with temperature above 19ºC, whereas *Prochlorococcus* and LNA prokaryotes showed a nearly sigmoid curve relationship with a transition between ca. 16 ºC and 25 ºC (Figure 4). The relationship between the biomass of both *Synechococcus* and picoeukaryotes and temperature showed a negative trend until $\sim$20ºC, and remained relatively constant above this temperature. PAR was included in the models of all picoplankton groups except picoeukaryotes. Whereas the biomass of *Prochlorococcus* exhibited a saturation type relationship with PAR, heterotrophic prokaryotes and *Synechococcus* showed a linear positive relationship. Finally, only LNA prokaryotes, *Synechococcus* and picoeukaryotes exhibited statistically significant relationships with nitrate supply. This relationship was negative for LNA prokaryotes and *Synechococcus*, whereas picoeukaryotes showed a unimodal function, peaking at $\sim$1 mmol NO$_3$ m^{-2} d^{-1}. Nitrate flux was the

only factor selected in the models to predict the contribution of LNA prokaryotes to heterotrophic picoplankton biomass, and both the cyanobacteria to picoeukaryotes biomass ratio and the autotrophic to heterotrophic biomass ratio. This relationship was negative in the three models. Temperature was also negatively correlated with the contribution of LNA prokaryotes to heterotrophic biomass, and the ratio of autotrophic to heterotrophic biomass. Finally, PAR showed a positive correlation with
5   the contribution of LNA prokaryotes to heterotrophic biomass, and the cyanobacteria to picoeukaryotes biomass ratio.

3.3   Ecological niches for picoplankton groups

By using non-parametric kernel density functions, we investigated the overlapping in the ecological niches of the autotrophic and heterotrophic picoplankton subgroups defined by using the three variables previously considered together with surface nitrate concentration (Figure 5). Photic layer depth-integrated biomass of each picoplankton group was used for this analy-
10   sis. These results revealed three ecological niches in the distribution of picoplankton subgroups. *Prochlorococcus* and LNA prokaryotes were more abundant in warm waters, where nitrate supply was low. HNA prokaryotes and *Synechococcus* dominated in cooler regions with medium to high nitrate supply, and picoeukaryotes were more abundant in cold waters with high nitrate supply. A large degree of overlapping of the ecological niches for all picoplankton subgroups was observed when only surface light was considered. For each picoplankton subgroup Table 4 shows the partial weighted overlap of the ecological
15   niches defined by the four factors: SST, PAR, nitrate flux and surface nitrate concentration. According to these data only nitrate supply enabled a statistically significant separation of the niches of both heterotrophic (HNA and LNA prokaryotes), and autotrophic (*Prochlorococcus*, *Synechococcus* and picoeukaryotes) picoplankton subgroups. Although the minimum overlap between *Prochlorococcus* and the other autotrophic picoplankton subgroups was also well defined by temperature, only nitrate supply could statistically distinguish the niche partitioning between the two groups of heterotrophic prokaryotes (p<0.05) and
20   between *Synechococcus* and picoeukariotes (p<0.1).

4   Discussion

4.1   Environmental factors and ecological niches

Picoplankton community composition and concurrent estimates of nitrate supply into the euphotic zone from highly contrasting marine environments allowed us to conclude that sea surface temperature and nitrate supply are the main factors controlling
25   the variability in the biomass of different subgroups, whereas surface light generally played a minor role. As far as we know, only one study had previously investigated the role of these environmental factors in the distribution of, in this case, the two major groups of cyanobacteria. By using a large flow cytometry dataset from all major ocean regions, Flombaum et al. (2013) concluded that temperature and light were the most important predictors of the abundances of *Prochlorococcus* and *Synechococcus*, with nitrate availability exerting a negligible effect. Although this conclusion seems to be contradictory with the
30   results presented here, some important differences between these studies should be noted. Firstly, Flombaum et al. (2013) used bulk estimates of seawater nitrate concentration as a proxy for nitrate availability in the euphotic zone. However, in near steady-

state systems such as the subtropical gyres, where diffusive nutrient supply into the euphotic zone is slow, nitrate concentrations are kept close to the detection limit due to phytoplankton uptake. For this reason, nitrate concentrations and actual nitrate supply into the euphotic zone in the vast oligotrophic regions are often largely disconnected Mouriño-Carballido et al. (2011, 2016). Moreover, whereas Flombaum et al. (2013) used *Prochlorococcus* and *Synechococcus* abundances determined at several depths in the upper 200 m, we used depth-integrated biomass of both autotrophic and heterotrophic picoplankton subgroups in the photic layer.

Although our results point to both temperature and nitrate supply as important factors controlling the distribution of the picoplankton subgroups (Figure 4 and Table 3), nitrate supply was the only factor that allowed the distinction between the ecological niches of autotrophic and heterotrophic picoplankton subgroups (Figure 5 and Table 4). Our attempt to sort out the ecological niches of picoplankton subgroups gave rise to three distinct categories. *Prochlorococcus* and LNA prokaryotes were more abundant in warmer waters (above 20ºC) where the availability of nitrate was low. *Synechococcus* and HNA prokaryotes prevailed mainly in cooler (below 20ºC) marine environments characterized by intermediate and high levels of nitrate supply, and finally, the niche for picoeukaryotes was characterized by low temperatures and high nitrate supply. These results underline the physiological and ecological features of the distinct picoplankton functional subgroups. Our results confirm the previously reported ecological differences between the two major groups of unicellular cyanobacteria (Scanlan and West, 2002; Partensky and Garczarek, 2010; Li, 2009).

Moreover, the ecological niche alignment of the two cyanobacteria genera with the two heterotrophic prokaryotes subgroups is consistent with taxa that prevail in oligotrophic regions (e.g. SAR11) being included in the LNA prokaryotes, whereas copiotrophic and more diverse taxa (Gammaproteobacteria, Bacteroidetes/Flavobacteria, etc) are generally grouped under HNA (Vila-Costa et al., 2012; Schattenhofer et al., 2011). Although the relationship between stratification, mixing and nutrient supply is not obvious (Mouriño-Carballido et al., 2016), our results are in general consistent with the patterns described by Bouman et al. (2011). These authors, by using vertical density stratification as a proxy for the three main environmental factors influencing phytoplankton growth (temperature, light and nutrients) in subtropical regions of the Pacific, Atlantic and Indian Oceans, described the dominance of photosynthetic picoeukaryotes in well-mixed waters, and the prevalence of cyanobacteria in strongly stratified conditions.

4.2 Physiological traits of picoplankton subgroups

Although previous studies have revealed that *Prochlorococcus* may have acquired the ability to use nitrate by horizontal gene transfer, their photosynthetic activity primarily relies on regenerated forms of nitrogen (Moore et al., 2002; Malmstrom et al., 2013). Our results support this view and substantiate that, after controlling for the concurrent effects of light and seawater temperature, *Prochlorococcus* biomass was uncorrelated with nitrate fluxes. However, it is important to note that we could not discriminate between high-light (HL) and low-light (LL) ecotypes, and that the presence of nitrate reductase seems to be more relevant in LL (Martiny et al., 2009; Berube et al., 2014). Evolutionary adaptation to light limiting conditions makes *Prochlorococcus* the most efficient light harvesters among Earth's photosynthetic organisms (Morel et al., 1993). Their competitive ability under light limiting conditions could explain the negative effect of light as a predictor for *Prochlorococcus* biomass.

Ultimately, the photo-physiological strategy of *Prochlorococcus* leads to i) thermal sensitivity of photosystem II (Mackey et al., 2013), which limits its fundamental niche to temperatures greater than 15 °C (Moore et al., 1995), and ii) high sensitivity to ultraviolet (UV) radiation in surface waters (Llabrés et al., 2010; Mackey et al., 2013; Sommaruga et al., 2005). This could explain that, after removing the effect of light, our data analysis revealed that the effect of temperature on *Prochlorococcus*
5   biomass showed a sigmoid relationship as temperature increased.

Synechococcus is able to use both new and regenerated forms of nitrogen (Moore et al., 2002; Mulholland and Lomas, 2008), which largely explains its wider geographical distribution range (Flombaum et al., 2013). The fact that it is more abundant at intermediate levels of nitrate supply is consistent with the lower intracellular nitrogen quota of *Synechococcus* relative to *Prochlorococcus*, and hence their higher growth rate under saturating nutrient conditions (Marañón et al., 2013). On the other
10   hand, the large affinity of *Prochlorococcus* to acquire nutrients (Partensky and Garczarek, 2010) and absorb light under severe nutrient- and light-limiting conditions (Mella-Flores et al., 2012), preclude the supremacy of *Synechococcus* in warm and stratified oligotrophic systems (Moore et al., 2007). Although *Prochlorococcus* and *Synechococcus* are not very different in cell size and they usually coexist in oligotrophic regions, differences in adaptation to light conditions and UV-stress lead to segregate their maximal distributions across space (vertical segregation) and through time (Chisholm, 1992; Mella-Flores et al.,
15   2012).

Picoeukaryotes, like *Synechococcus*, also exhibited a negative relationship with seawater temperature, again reflecting the superior competitive ability of *Prochlorococcus* under severe nutrient-limiting conditions (Moore et al., 2007). The relative dominance of cyanobacteria in oligotrophic systems results from the fact that cyanobacteria are less negatively affected by nutrient diffusion limitation than picoeukaryotes (Chisholm, 1992). It is widely accepted that small cells are at an advantage
20   over large cells in stratified open ocean environments, where nutrient recycling dominates biogeochemical fluxes (Raven, 1998). First, the surface-to-volume ratio increases with decreasing cell size, which narrows the nutrient diffusion boundary layer around the cell and facilitates the acquisition of nutrients in nutrient impoverished environments. Second, small-sized cells have lower sinking rates than their larger counterparts, which allow them to extend their chances of survival in the euphotic layer (Smayda, 1980; Chisholm, 1992; Kiørboe, 1993).

25   Our analysis indicates that among the picophytoplankton, picoeukaryotes were the most responsive to nutrient fluxes. This is consistent with experimental observations under laboratory-controlled conditions revealing that, within the picoplankton size range, the maximum attainable growth rate increases with increasing cell size (Raven, 1994; Marañón et al., 2013). This positive relationship between maximum growth rate and cell size in the pico- to small nano-phytoplankton size range has been explained as a trade-off between intracellular nitrogen quotas (N requirements) and mass-specific nitrate uptake rates (N uptake)
30   (Marañón et al., 2013). Whereas nitrogen uptake rate exhibits an isometric relationship with cell size, smaller picoplankton cells have substantially larger intracellular nitrogen quotas, which reduce their capability to maximize carbon-specific growth rates. On the other hand high maximum growth rates represent an advantage for picoeukaryotes, as to any other organism, as they attenuate the effect of loss processes such as predation or the wash-out of plankton communities in highly dynamic, turbulent systems (Sherr et al., 2005; Echevarría et al., 2009). For instance, the microzooplankton is thought to maintain the

biomass of their prey under tight control, and thus slight variations in picophytoplankton growth rate may substantially alter the resulting biomass of the different picophytoplankton subgroups (Chen et al., 2009).

The unimodal relationship observed between the biomass of picoeukaryotes and nitrate supply (Figure 4) could seem at first contradictory with the rising hypothesis proposed by Barber and Hiscock (2006), which describes that improved growth condi-

5 tions benefit all phytoplankton size-classes, including picoplankton. In this regard, Brewin et al. (2014) by using data collected along the Atlantic Meridional Transect cruises showed that <2 µm size-fractionated chlorophyll was positively correlated with total chlorophyll only until a value of 1 mg m^{-3}, and then it did not show any positive relationship with total chlorophyll. It is also important to note that surface abundance of picoplankton subgroups reported in our study, which are consistent with previous observations (Zubkov et al., 2000; Frojan et al., 2014; Teira et al., 2015), did show higher surface abundance of pi-

10 coeukaryotes in the Galicia coastal upwelling and the Mediterranean compared to the tropical and subtropical Atlantic (Table 2 and Figure A3). However, this pattern was diluted when depth-integrated biomasses were computed as the lower limit for the integration (the base of the photic zone) was much shallower in the coastal upwelling domain (ca. 37 m), compared to the Mediterranean (ca. 62 m) and the tropical and subtropical regions (ca. 109 m).

Heterotrophic prokaryotes also use dissolved inorganic nutrients, including nitrate, for growth (Kirchman, 2000). Consistent

15 with this, Gasol et al. (2009) showed a positive relationship between prokaryotic abundance and a proxy for nutrient supply in a latitudinal gradient across the Atlantic. They did not partition this effect on the two subgroups that can universally be differentiated among bacteria and archaea. Our results suggest that LNA prokaryotes respond less markedly to nutrient fluxes than HNA prokaryotes. The effect of nitrate supply on the biomass of LNA prokaryotes showed a linear negative relationship as nitrate supply increases, perhaps associated with their ability to survive under nutrient starving conditions (Mary et al.,

20 2008). Under such conditions, proteorhodopsin-containing LNA prokaryotes (e.g. example SAR11) can use energy from light (Mary et al., 2008; Pinhassi et al., 2016) improving their competitiveness against non-proteorhodopsin-containing prokaryotes. Consistent with this idea, our results showed a positive relationship between the biomass of LNA prokaryotes and PAR. Li et al. (2004) already proposed the ubiquity of this bottom-up control of prokaryotic abundance in oligotrophic environments (<1 mg Chl m^3). Therefore, we believe that it is more the difference in the suite of genes (Schattenhofer et al., 2011) than in

25 cell size (Morán et al., 2015) the underlying cause for the clear niche difference between LNA and HNA prokaryotes.

5 Outlook

Picoplankton often dominate marine phytoplankton biomass and primary production in oligotrophic regions (Chisholm, 1992; Agawin et al., 2000), contribute overwhelmingly to the recycling of organic matter (Azam et al., 1983; Fenchel, 2008), and could have a substantial contribution to the export of carbon to the deep ocean (Richardson and Jackson, 2007). However,

30 our limited understanding about the factors that control picoplankton community composition constrains our ability to include them in ocean biogeochemical models, and predict the consequences of future global change scenarios. For the first time, by combining observations which allowed us to estimate vertical nutrient fluxes, instead of nitrate concentrations, we investigated the role of temperature, light and nitrate supply in the distribution of the major autotrophic and heterotrophic picoplankton

subgroups. Our results highlight the role of nitrate supply in the distribution of picoplankton subgroups, as it was the only factor that allowed the statistically significant distinction of the ecological niches between the autotrophic and heterotrophic picoplankton subgroups. In general, autotrophic picoplankton biomass was dominated by *Prochlorococcus* in warmer waters where the availability of nitrate was low, and by *Synechococcus* and picoeukaryotes in cooler waters with medium to high nitrate availability. Similarly, LNA prokaryotes dominated heterotrophic picoplankton biomass in regions of weak nitrate supply, whereas HNA prokaryotes dominated the heterotrophic community in regions of enhanced nutrient supply. Although our study included 97 stations sampled in contrasting environments, a larger dataset, including a broader range of environmental conditions, will be needed to accurately discern the role of temperature and nitrate supply in the field, as both factors are strongly correlated in the ocean. In this regard, by growing three phytoplankton species (the diatom *Skeletonema costatum*, the coccolithophore *Emiliania huxleyi* and the picocyanobacteria *Synechococcus* spp.) in the lab, Marañón et al. (2018) showed a reduced sensitivity of metabolic rates to temperature variability under nutrient-depleted conditions, suggesting that nutrient availability controls the temperature dependence of metabolism. Consistent with these results, our statistical analyses stress the relevance of nitrate supply in the distinction of the ecological niches of heterotrophic and autotrophic picoplankton subgroups. Other mechanisms of nutrient supply, such as mesoscale and sub-mesoscale turbulence, atmospheric deposition, nitrogen fixation and more complex 3-dimensional dynamics Jenkins and Doney (2003); Bonnet et al. (2005); Estrada et al. (2014); Fernández-Castro et al. (2015), as well as the influence of trophic interactions Van Mooy et al. (2006); Baudoux et al. (2007); Chen et al. (2009); Rusch et al. (2010) deserve further investigation.

According to our results, in a future ocean where global change scenarios predict an increase in surface temperature and stratification (Howes et al., 2015), the resulting decrease in nitrate supply into the euphotic zone (Lewandowska et al., 2014) would lead to the dominance of autotrophic picoplankton by cyanobacteria, whereas the picoeukaryotes would decrease their contribution. Due to the smaller contribution of cyanobacteria to the transfer of carbon to the deep ocean compared to picoeukaryotes, this pattern could have important implications in the efficiency of the biological carbon pump (Corno et al., 2007).

Author contributions. JO., PC and BM. designed the research; JO. analyzed the data and JO. and BM. prepared the manuscript with contributions from all the co-authors.

Competing interests. The authors declare no conflict of interest.

Acknowledgements. We thank the officers and crew of the R/V Hespérides, Sarmiento de Gamboa, Mytilus, Ramon Margalef and Lura for their help during the cruises. We are also very grateful to Fátima Eiroa for the flow cytometry analysis in NICANOR, HERCULES1,

HERCULES2, HERCULES3 and ASIMUTH cruises. Finally, we would like to thank Julia Uitz and two anonymous reviewers for their valuable comments on the manuscript.

This research was supported by the Spanish Ministry of Economy and Competitiveness (MINECO) through projects: CTM2012-30680 to Beatriz Mouriño, CTM2008-0626I-C03-01 to Mikel Latasa, REN2003-09532-C03-01 to Ramiro Varela Benvenuto, CTM2004-05174-C02 to Emilio Marañón, CTM2011-25035 to Pedro Cermeño, by the Galician Goverment through grants 09MMA027604PR to Manuel Ruiz Villareal, and EM2013/021 to Beatriz Mouriño, by the Instituto Español de Oceanografia (IEO) through the time-series project RADIALES coordinated by Antonio Bode and by the 7th Framework Programme of the European Commision through grants FP7 SPACE.2010.1.1-01 261860 to Manuel Ruiz Villareal. Jose Luis Otero Ferrer acknowledges the receipt of a FPI contract from MINECO (CTM2012-30680), and Bieito Fernández Castro a Juan de La Cierva Formación fellowship (FJCI-641 2015-25712, Ministerio de Economía y Competitividad, Spanish Goverment).

References

Agawin, N. S., Duarte, C. M., and Agustí, S.: Nutrient and temperature control of the contribution of picoplankton to phytoplankton biomass and production, Limnology and Oceanography, 45, 591–600, 2000.

Álvarez-Salgado, X. A., Roson, G., Perez, F. F., and Pazos, Y.: Hydrographic variability off the Rías Baixas (NW Spain) during the upwelling season, JOURNAL OF GEOPHYSICAL RESEARCH, 98455, 447–14, https://doi.org/10.1029/93JC00458, 1993.

Alvarez-Salgado, X. A., Borges, A. V., Figueiras, F. G., and Chou, L.: Iberian margin: the Rías, in: Carbon and Nutrient Fluxes in Continental Margins: A Global Synthesis, pp. 103–120, IGBP, 2010.

Aranguren-Gassis, M., Serret, P., Fernández, E., Herrera, J. L., Domínguez-Yanes, J. F., Pérez, V., and Escánez, J.: Production and respiration control the marine microbial metabolic balance in the eastern North Atlantic subtropical gyre, Deep Sea Research Part I: Oceanographic Research Papers, 58, 768–775, https://doi.org/10.1016/j.dsr.2011.05.003, 2011.

Azam, F., Fenchel, T., Field, J. G., Gray, J. C. S., Meyer-Reil, L. A., and Thingstad, F.: The ecological role of water-column microbes in the sea., Marine Ecology Progress Series, 10, 257–263, https://doi.org/10.3354/meps010257, 1983.

Barber, R. T. and Hiscock, M. R.: A rising tide lifts all phytoplankton: Growth response of other phytoplankton taxa in diatom-dominated blooms, Global Biogeochemical Cycles, 20, n/a–n/a, https://doi.org/10.1029/2006GB002726, 2006.

Barton, A. D., Ward, B. A., Williams, R. G., and Follows Michael J.: The impact of fine-scale turbulence on phytoplankton community structure, Limnology & Oceanography: Fluids & Environments, 4, 34–49, http://lofe.dukejournals.org/content/4/34.full, 2014.

Barton, A. D., Lozier, M. S., and Williams, R. G.: Physical controls of variability in north Atlantic phytoplankton communities, Limnology and Oceanography, 60, 181–197, https://doi.org/10.1002/lno.10011, 2015.

Baudoux, A.-C., Veldhuis, M. J. W., Witte, H. J., and Brussaard, C. P. D.: Viruses as mortality agents of picophytoplankton in the deep chlorophyll maximum layer during IRONAGES III, Limnology and Oceanography, 52, 2519–2529, https://doi.org/10.4319/lo.2007.52.6.2519, http://doi.wiley.com/10.4319/lo.2007.52.6.2519, 2007.

Berube, P. M., Biller, S. J., Kent, A. G., Berta-Thompson, J. W., Roggensack, S. E., Roache-Johnson, K. H., Ackerman, M., Moore, L. R., Meisel, J. D., Sher, D., Thompson, L. R., Campbell, L., Martiny, A. C., and Chisholm, S. W.: Physiology and evolution of nitrate acquisition in Prochlorococcus., The ISME journal, pp. 1–13, https://doi.org/10.1038/ismej.2014.211, http://www.ncbi.nlm.nih.gov/pubmed/25350156, 2014.

Bonnet, S., Guieu, C., Chiaverini, J., Ras, J., and Stock, A.: Effect of atmospheric nutrients on the autotrophic communities in a low nutrient, low chlorophyll system, Limnology and Oceanography, 50, 1810–1819, https://doi.org/10.4319/lo.2005.50.6.1810, 2005.

Bouman, H. a., Ulloa, O., Barlow, R., Li, W. K., Platt, T., Zwirglmaier, K., Scanlan, D. J., and Sathyendranath, S.: Water-column stratification governs the community structure of subtropical marine picophytoplankton., Environmental microbiology reports, 3, 473–82, https://doi.org/10.1111/j.1758-2229.2011.00241.x, http://www.ncbi.nlm.nih.gov/pubmed/23761310, 2011.

Bouvier, T., Del Giorgio, P. A., and Gasol, J. M.: A comparative study of the cytometric characteristics of High and Low nucleic-acid bacterioplankton cells from different aquatic ecosystems, Environmental Microbiology, 9, 2050–2066, https://doi.org/10.1111/j.1462-2920.2007.01321.x, 2007.

Brewin, R. J. W., Sathyendranath, S., Tilstone, G., Lange, P. K., and Platt, T.: Amulticomponent model of phytoplankton size structure, Journal of Geophysical Research: Oceans, 119, 1–19, https://doi.org/10.1002/2014JC009859.Received, 2014.

Buitenhuis, E. T., Li, W. K., Vaulot, D., Lomas, M. W., Landry, M. R., Partensky, F., Karl, D. M., Ulloa, O., Campbell, L., Jacquet, S., Lantoine, F., Chavez, F. P., Macias, D., Gosselin, M., and McManus, G. B.: Picophytoplankton biomass distribution in the global ocean, Earth System Science Data, 4, 37–46, https://doi.org/10.5194/essd-4-37-2012, 2012.

Calvo-Díaz, A. and Morán, X. A. G.: Seasonal dynamics of picoplankton in shelf waters of the southern Bay of Biscay, Aquatic Microbial Ecology, 42, 159–174, https://doi.org/10.3354/ame042159, 2006.

Cermeño, P., Choucino, P., Fernández-Castro, B., Figueiras, F. G., Marañón, E., Marrasé, C., Mouriño-Carballido, B., Pérez-Lorenzo, M., Rodríguez-Ramos, T., Teixeira, I. G., and Vallina, S. M.: Marine Primary Productivity Is Driven by a Selection Effect, Frontiers in Marine Science, 3, 173, https://doi.org/10.3389/fmars.2016.00173, http://journal.frontiersin.org/article/10.3389/fmars.2016.00173, 2016.

Chen, B., Liu, H., Landry, M. R., Chen, M., Sun, J., Shek, L., Chen, X., and Harrison, P. J.: Estuarine nutrient loading affects phytoplankton growth and microzooplankton grazing at two contrasting sites in Hong Kong coastal waters, Marine Ecology Progress Series, 379, 77–90, https://doi.org/10.3354/meps07888, 2009.

Chisholm, S. W.: Phytoplankton Size, in: Primary Productivity and Biogeochemical Cycles in the Sea, edited by Falkowski, P. G., Woodhead, A. D., and Vivirito, K., pp. 213–237, Springer US, Boston, MA, https://doi.org/10.1007/978-1-4899-0762-2_12, http://dx.doi.org/10.1007/978-1-4899-0762-2_12, 1992.

Corno, G., Karl, D. M., Church, M. J., Letelier, R. M., Lukas, R., Bidigare, R. R., and Abbott, M. R.: Impact of climate forcing on ecosystem processes in the North Pacific Subtropical Gyre, Journal of Geophysical Research, 112, C04 021, https://doi.org/10.1029/2006JC003730, http://doi.wiley.com/10.1029/2006JC003730, 2007.

Echevarría, F., Zabala, L., Corzo, A., Navarro, G., Prieto, L., and Macías, D.: Spatial distribution of autotrophic picoplankton in relation to physical forcings: The Gulf of Cádiz, Strait of Gibraltar and Alborán Sea case study, Journal of Plankton Research, 31, 1339–1351, https://doi.org/10.1093/plankt/fbp070, 2009.

Espinoza-González, O., Figueiras, F. G., Crespo, B. G., Teixeira, I. G., and Castro, C. G.: Autotrophic and heterotrophic microbial plankton biomass in the NW Iberian upwelling: seasonal assessment of metabolic balance, Aquatic Microbial Ecology, 67, 77–89, https://doi.org/10.3354/ame01584, 2012.

Estrada, M., Latasa, M., Emelianov, M., Gutiérrez-Rodríguez, A., Fernández-Castro, B., Isern-Fontanet, J., Mouriño-Carballido, B., Salat, J., and Vidal, M.: Seasonal and mesoscale variability of primary production in the deep winter-mixing region of the NW Mediterranean, Deep-Sea Research Part I: Oceanographic Research Papers, 94, 45–61, https://doi.org/10.1016/j.dsr.2014.08.003, http://dx.doi.org/10.1016/j.dsr.2014.08.003, 2014.

Fenchel, T.: The microbial loop - 25 years later, Journal of Experimental Marine Biology and Ecology, 366, 99–103, https://doi.org/10.1016/j.jembe.2008.07.013, 2008.

Fernández, E., Álvarez-Salgado, X. A., Beiras, R., Ovejero, A., and Méndez, G.: Coexistence of urban uses and shellfish production in an upwelling-driven, highly productive marine environment: The case of the Ría de Vigo (Galicia, Spain), Regional Studies in Marine Science, 8, 362–370, https://doi.org/10.1016/j.rsma.2016.04.002, http://dx.doi.org/10.1016/j.rsma.2016.04.002, 2016.

Fernández-Castro, B., Mouriño-Carballido, B., Marañón, E., Choucino, P., Gago, J., Ramírez, T., Vidal, M., Bode, A., Blasco, D., Royer, S.-J., Estrada, M., and Simó, R.: Importance of salt fingering for new nitrogen supply in the oligotrophic ocean, Nature Communications, In press, 1–10, https://doi.org/10.1038/ncomms9002, 2015.

Fernández-Castro, B., Gilcoto, M., Naveira-Garabato, A. C., Villamaña, M., Graña, R., and Mouriño-Carballido, B.: Modulation of the Semidiurnal Cycle of Turbulent Dissipation by Wind-Driven Upwelling in a Coastal Embayment, Journal of Geophysical Research: Oceans, 123, 4034–4054, https://doi.org/10.1002/2017JC013582, 2018.

Finkel, Z. V., Beardall, J., Flynn, K. J., Quigg, A., Rees, T. A. V., and Raven, J. A.: Phytoplankton in a changing world: Cell size and elemental stoichiometry, Journal of Plankton Research, 32, 119–137, https://doi.org/10.1093/plankt/fbp098, 2010.

Flombaum, P., Gordillo, R. A., Zabala, L. L., Jiao, N., Karl, D. M., Li, W. K., Lomas, M. W., Veneziano, D., Vera, C. S., Vrugt, J. A., and Martiny, A. C.: Present and future global distributions of the marine Cyanobacteria Prochlorococcus and Synechococcus, PNAS, 110, 1–12, https://doi.org/10.1073/pnas.1307701110/-/DCSupplemental.www.pnas.org/cgi/doi/10.1073/pnas.1307701110, 2013.

Fraga, F.: Upwelling off the Galician coast, northwest Spain, Coastal and Estuarine Sciences, 1, 176–182, https://doi.org/10.1029/CO001p0176, 1981.

Frojan, M., Arbones, B., Zuniga, D., Castro, C. G., and Figueiras, F. G.: Microbial plankton community in the Ria de Vigo (NW Iberian upwelling system): impact of the culture of Mytilus galloprovincialis, Marine Ecology Progress Series, 498, 43–U371, https://doi.org/10.3354/meps10612, 2014.

Gasol, J. M. and del Giorgio, P. A.: Using flow cytometry for counting natural planktonic bacteria and understanding the structure of planktonic bacterial communities, Scientia Marina, 64, 197–224, https://doi.org/10.3989/scimar.2000.64n2197, http://scientiamarina.revistas.csic.es/index.php/scientiamarina/article/viewArticle/755http://links.isiglobalnet2.com/gateway/Gateway.cgi?GWVersion=2&SrcAuth=mekentosj&SrcApp=Papers&DestLinkType=FullRecord&DestApp=WOS&KeyUT=000088019800007%5Cnpapers2://p, 2000.

Gasol, J. M., Vázquez-Domínguez, E., Vaqué, D., Agustí, S., and Duarte, C. M.: Bacterial activity and diffusive nutrient supply in the oligotrophic Central Atlantic Ocean, Aquatic Microbial Ecology, 56, 1–12, https://doi.org/10.3354/ame01310, http://www.int-res.com/abstracts/ame/v56/n1/p1-12/, 2009.

Geange, S. W., Pledger, S., Burns, K. C., and Shima, J. S.: A unified analysis of niche overlap incorporating data of different types, Methods in Ecology and Evolution, 2, 175–184, https://doi.org/10.1111/j.2041-210X.2010.00070.x, 2011.

Gomes, A., Gasol, J. M., Estrada, M., Franco-Vidal, L., Díaz-Pérez, L., Ferrera, I., and Morán, X. A. G.: Heterotrophic bacterial responses to the winter-spring phytoplankton bloom in open waters of the NW Mediterranean, Deep-Sea Research Part I: Oceanographic Research Papers, 96, 59–68, https://doi.org/10.1016/j.dsr.2014.11.007, http://dx.doi.org/10.1016/j.dsr.2014.11.007, 2015.

Grasshoff, K., Kremling, K., and Ehrhardt, M.: Methods of Seawater Analysis: Third, Completely Revised and Extended Edition, WILEY-VCH, https://doi.org/10.1002/9783527613984, 2007.

Grob, C., Ulloa, O., Li, W. K., Alarcón, G., Fukasawa, M., and Watanabe, S.: Picoplankton abundance and biomass across the eastern South Pacific Ocean along latitude 32.5°S, Marine Ecology Progress Series, 332, 53–62, https://doi.org/10.3354/meps332053, 2007.

Guasto, J. S., Rusconi, R., and Stocker, R.: Fluid Mechanics of Planktonic Microorganisms, Annual Review of Fluid Mechanics, 44, 373–400, https://doi.org/10.1146/annurev-fluid-120710-101156, http://www.annualreviews.org/doi/10.1146/annurev-fluid-120710-101156, 2012.

Guidi, L., Chaffron, S., Bittner, L., Eveillard, D., Larhlimi, A., Roux, S., Darzi, Y., Audic, S., Berline, L., Brum, J., Coelho, L. P., Espinoza, J. C. I., Malviya, S., Sunagawa, S., Dimier, C., Kandels-Lewis, S., Picheral, M., Poulain, J., Searson, S., Coordinators, T. O., Stemmann, L., Not, F., Hingamp, P., Speich, S., Follows Michael J., Karp-Boss, L., Boss, E., Ogata, H., Pesant, S., Weissenbach, J., Wincker, P., Acinas, S. G., Bork, P., de Vargas, C., Iudicone, D., Sullivan, M. B., Raes, J., Karsenti, E., Bowler, C., and Gorsky, G.: Plankton networks driving carbon export in the oligotrophic ocean, Nature, 532, in review, https://doi.org/10.1038/nature16942, http://dx.doi.org/10.1038/nature16942, 2015.

Gundersen, K., Heldal, M., Norland, S., Purpie, D. A., and Knap, A. N.: Elemental C, N, and P cell content of individual bacteria collected at the Bermuda Atlantic Time-series Study (BATS) site, Limnology and oceanography, 47, 1525–1530, http://cat.inist.fr/?aModele=afficheN&cpsidt=13918565, 2002.

Hastie, T. J. and Tibshirani, R.: Varying-coefficient Models, journal of the royal statistical society, 55, 757–796, https://doi.org/10.2307/2345993, 1993.

Howes, E. L., Joos, F., Eakin, C. M., and Gattuso, J.-P.: An updated synthesis of the observed and projected impacts of climate change on the chemical, physical and biological processes in the oceans, Frontiers in Marine Science, 2, https://doi.org/10.3389/fmars.2015.00036,
5   http://journal.frontiersin.org/Article/10.3389/fmars.2015.00036/abstract, 2015.

Hutchinson, G.: Concludig remarks, Cold Spring Harbor Symposia on Quantitative Biology, 22, 415–427, 1957.

Jenkins, W. J. and Doney, S. C.: The subtropical nutrient spiral, Global Biogeochemical Cycles, 17, 1110, https://doi.org/10.1029/2003GB002085, http://doi.wiley.com/10.1029/2003GB002085, 2003.

Johnson, Z. I., Zinser, E. R., Coe, A., McNulty, N. P., Woodward, E. M. S., and Chisholm, S. W.: Niche partitioning among Prochlorococcus
10   ecotypes along ocean-scale environmental gradients., Science (New York, N.Y.), 311, 1737–40, https://doi.org/10.1126/science.1118052, http://www.ncbi.nlm.nih.gov/pubmed/16556835, 2006.

Kark, S., Mukerji, T., Safriel, U. N., Noy-Meir, I., Nissani, R., and Darvasi, A.: Peak morphological diversity in an ecotone unveiled in the chukar partridge by a novel Estimator in a Dependent Sample (EDS), Journal of Animal Ecology, 71, 1015–1029, https://doi.org/10.1046/j.1365-2656.2002.00665.x, 2002.

15 Karp-Boss, L., Boss, E., and Jumars, P.: Nutrient fluxes to planktonic osmotrophs in the presence of fluid motion, Oceanography and Marine Biology, 34, 71–107, http://citeseerx.ist.psu.edu/viewdoc/download?doi=10.1.1.473.2266&rep=rep1&type=pdf, 1996.

Kiørboe, T.: Turbulence, Phytoplankton Cell Size, and the Structure of Pelagic Food Webs, Advances in Marine Biology, 29, 1–72, https://doi.org/10.1016/S0065-2881(08)60129-7, 1993.

Kirchman, D. L.: Uptake and regeneration of inorganic nutrients by marine heterotrophic bacteria, Microbial ecology of the oceans, pp.
20   261–288, 2000.

Kirk, J. T.: Light and photosynthesis in aquatic ecosystems, Cambridge University Press, 1994.

Laufkötter, C., Vogt, M., Gruber, N., Aumont, O., Bopp, L., Doney, S. C., Dunne, J. P., Hauck, J., John, J. G., Lima, I. D., Seferian, R., and Völker, C.: Projected decreases in future marine export production: The role of the carbon flux through the upper ocean ecosystem, Biogeosciences, 13, 4023–4047, https://doi.org/10.5194/bg-13-4023-2016, 2016.

25 Lazier, J. R. and Mann, K. H.: Turbulence and the diffusive layers around small organisms, Deep Sea Research Part A, Oceanographic Research Papers, 36, 1721–1733, https://doi.org/10.1016/0198-0149(89)90068-X, 1989.

Lewandowska, A. M., Boyce, D. G., Hofmann, M., Matthiessen, B., Sommer, U., and Worm, B.: Effects of sea surface warming on marine plankton, Ecology Letters, 17, 614–623, https://doi.org/10.1111/ele.12265, 2014.

Li, W.: Macroscopic patterns in marine plankton, in: Encyclopedia of biodiversity, edited by Levin, S. A., pp. 667–680, Academic
30   Press, https://doi.org/http://dx.doi.org/10.1016/B978-0-12-384719-5.00291-4, http://enviro.doe.gov.my/lib/digital/1385476065-3-s2.0-B9780122268656005821-main.pdf, 2007.

Li, W. K.: Macroecological patterns of phytoplankton in the northwestern North Atlantic Ocean, Nature, 419, 154–157, https://doi.org/10.1038/nature00983.1., 2002.

Li, W. K.: Plankton populations and communities, Marine Macroecology, pp. 29–64, 2009.

35 Li, W. K., Jellett, J. F., and Dickie, P. M.: DNA distributions in planktonic bacteria stained with TOTO or TO-PRO, Limnology and Oceanography, 40, 1485–1495, https://doi.org/10.4319/lo.1995.40.8.1485, 1995.

Li, W. K., Head, E. J. H., and Harrison, W. G.: Macroecological limits of heterotrophic bacterial abundance inthe ocean, Deep Sea Research Part I: Oceanographic Research Papers, 51, 1529–1540, 2004.

Llabrés, M., Agustí, S., Alonso-Laita, P., and Herndl, G. J.: Synechococcus and Prochlorococcus cell death induced by UV radiation and the penetration of lethal UVR in the Mediterranean Sea, Marine Ecology Progress Series, 399, 27–37, https://doi.org/10.3354/meps08332, 2010.

Lomas, M. W. and Moran, S. B.: Evidence for aggregation and export of cyanobacteria and nano-eukaryotes from the Sargasso Sea euphotic zone, Biogeosciences, 8, 203–216, https://doi.org/10.5194/bg-8-203-2011, 2011.

Mackey, K. R. M., Paytan, A., Caldeira, K., Grossman, A. R., Moran, D., McIlvin, M., and Saito, M. A.: Effect of temperature on photosynthesis and growth in marine Synechococcus spp., Plant physiology, 163, 815–29, https://doi.org/10.1104/pp.113.221937, http://www.pubmedcentral.nih.gov/articlerender.fcgi?artid=3793060&tool=pmcentrez&rendertype=abstract, 2013.

Malmstrom, R. R., Rodrigue, S., Huang, K. H., Kelly, L., Kern, S. E., Thompson, A., Roggensack, S. E., Berube, P. M., Henn, M. R., and Chisholm, S. W.: Ecology of uncultured Prochlorococcus clades revealed through single-cell genomics and biogeographic analysis, ISME Journal, 7, 184–198, https://doi.org/10.1038/ismej.2012.89, 2013.

Marañón, E.: Cell Size as a Key Determinant of Phytoplankton Metabolism and Community Structure., Annual Review of Marine Science, 7, 241–64, https://doi.org/10.1146/annurev-marine-010814-015955, http://www.ncbi.nlm.nih.gov/pubmed/25062405, 2015.

Marañón, E., Cermeño, P., López-Sandoval, D. C., Rodríguez-Ramos, T., Sobrino, C., Huete-Ortega, M., Blanco, J. M., and Rodríguez, J.: Unimodal size scaling of phytoplankton growth and the size dependence of nutrient uptake and use., Ecology letters, 16, 371–9, https://doi.org/10.1111/ele.12052, http://www.ncbi.nlm.nih.gov/pubmed/23279624, 2013.

Marañón, E., Lorenzo, M. P., Cermeño, P., and Mouriño-carballido, B.: Nutrient limitation suppresses the temperature dependence of phytoplankton metabolic rates, The ISME Journal, https://doi.org/10.1038/s41396-018-0105-1, http://dx.doi.org/10.1038/s41396-018-0105-1, 2018.

Marie, D. and Partensky, F.: Analyse de micro-organismes marins, in: La cytométrie en flux, edited by RONOT, X., GRUNWALD, D., MAYOL, J.-F., and BOUTONNAT, J., pp. 211–233, Lavoisier, 2006.

Marra, G. and Wood, S. N.: Coverage Properties of Confidence Intervals for Generalized Additive Model Components, Scandinavian Journal of Statistics, 39, 53–74, https://doi.org/10.1111/j.1467-9469.2011.00760.x, 2012.

Martiny, A. C., Kathuria, S., and Berube, P. M.: Widespread metabolic potential for nitrite and nitrate assimilation among Prochlorococcus ecotypes., Proceedings of the National Academy of Sciences of the United States of America, 106, 10787–92, https://doi.org/10.1073/pnas.0902532106, http://www.pubmedcentral.nih.gov/articlerender.fcgi?artid=2705535&tool=pmcentrez&rendertype=abstract, 2009.

Mary, I., Tarran, G. A., Warwick, P. E., Terry, M. J., Scanlan, D. J., Burkill, P. H., and Zubkov, M. V.: Light enhanced amino acid uptake by dominant bacterioplankton groups in surface waters of the Atlantic Ocean, FEMS Microbiology Ecology, 63, 36–45, https://doi.org/10.1111/j.1574-6941.2007.00414.x, 2008.

Mella-Flores, D., Six, C., Ratin, M., Partensky, F., Boutte, C., Le Corguillé, G., Marie, D., Blot, N., Gourvil, P., Kolowrat, C., and Garczarek, L.: Prochlorococcus and Synechococcus have Evolved Different Adaptive Mechanisms to Cope with Light and UV Stress., Frontiers in microbiology, 3, 285, https://doi.org/10.3389/fmicb.2012.00285, http://www.pubmedcentral.nih.gov/articlerender.fcgi?artid=3441193&tool=pmcentrez&rendertype=abstract, 2012.

Moore, L. R., Goericke, R., and Chisholm, S. W.: Comparative physiology of Synechococcus and Prochlorococcus: influence of light and temperature on growth, pigments, fluorescence and absorptive, Marine Ecology Progress Series, 116, 259–275, http://chisholmlab.mit.edu/publications/1995_Moore_Goericke_C_Comp_phys_Syn_Pro_light_temp.pdf, 1995.

Moore, L. R., Post, A. F., Rocap, G., and Chisholm, S. W.: Utilization of different nitrogen sources by the marine cyanobacteria Prochlorococcus and Synechococcus, Limnology and Oceanography, 47, 989–996, https://doi.org/10.4319/lo.2002.47.4.0989, http://www.aslo.org/lo/toc/vol_47/issue_4/0989.html, 2002.

Moore, L. R., Coe, A., Zinser, E. R., Saito, M. A., Sullivan, M. B., Lindell, D., Frois-Moniz, K., Waterbury, J. B., and Chisholm, S. W.: Culturing the marine cyanobacterium Prochlorococcus, Limnology and Oceanography: Methods, 5, 353–362, https://doi.org/10.4319/lom.2007.5.353, http://doi.wiley.com/10.4319/lom.2007.5.353, 2007.

Morán, X. A. G.: Annual cycle of picophytoplankton photosynthesis and growth rates in a temperate coastal ecosystem: A major contribution to carbon fluxes, Aquatic Microbial Ecology, 49, 267–279, https://doi.org/10.3354/ame01151, 2007.

Morán, X. A. G., Alonso-Sáez, L., Nogueira, E., Ducklow, H. W., González, N., López-Urrutia, , Díaz-Pérez, L., Calvo-Díaz, A., Arandia-Gorostidi, N., and Huete-Stauffer, T. M.: More, smaller bacteria in response to ocean's warming?, Proceedings of the Royal Society B: Biological Sciences, 282, https://doi.org/10.1098/rspb.2015.0371, 2015.

Moreira-Coello, V., Mouriño-Carballido, B., Marañón, E., Chouciño, P., Fernández, A., Varela, M., and Bode, A.: Biological N2 fixation in the upwelling region off NW Iberia: magnitude, relevance and main players, Frontiers in Marine Science, 4, http://journal.frontiersin.org/article/10.3389/fmars.2017.00303/abstract, 2017.

Morel, A., Ahn, Y.-H., Partensky, F., Vaulot, D., and Claustre, H.: Prochlorococcus and Synechococcus: A comparative study of their optical properties in relation to their size and pigmentation, Journal of Marine Research, 51, 617–649, http://www.ingentaconnect.com/content/jmr/jmr/1993/00000051/00000003/art00008, 1993.

Morel, A., Huot, Y., Gentili, B., Werdell, P. J., Hooker, S. B., and Franz, B. a.: Examining the consistency of products derived from various ocean color sensors in open ocean (Case 1) waters in the perspective of a multi-sensor approach, Remote Sensing of Environment, 111, 69–88, https://doi.org/10.1016/j.rse.2007.03.012, http://linkinghub.elsevier.com/retrieve/pii/S0034425707001307, 2007.

Mouillot, D., Stubbs, W., Faure, M., Dumay, O., Tomasini, J. A., Wilson, J. B., and Chi, T. D.: Niche overlap estimates based on quantitative functional traits: A new family of non-parametric indices, Oecologia, 145, 345–353, https://doi.org/10.1007/s00442-005-0151-z, 2005.

Mouriño-Carballido, B., Graña, R., Fernández, A., Bode, A., Varela, M., Domínguez-Yanes, J. F., Escánez, J., de Armas, D., and Marañón, E.: Importance of N2 fixation vs. nitrate eddy diffusion along a latitudinal transect in the Atlantic Ocean, Limnology and Oceanography, 56, 999–1007, https://doi.org/10.4319/lo.2011.56.3.0999, http://www.aslo.org/lo/toc/vol_56/issue_3/0999.html, 2011.

Mouriño-Carballido, B., Hojas, E., Cermeño, P., Chouciño, P., Fernández-Castro, B., Latasa, M., Marañón, E., Morán, X. A. G., and Vidal, M.: Nutrient supply controls picoplankton community structure during three contrasting seasons in the northwestern Mediterranean Sea, Marine Ecology Progress Series, 543, 1–19, https://doi.org/10.3354/meps11558, 2016.

Mulholland, M. R. and Lomas, M. W.: Nitrogen uptake and assimilation, in: Nitrogen in the Marine Environment, edited by Capone, D., Bronk, D., Mulholl, M., and Carpenter, E., pp. 303–384, Elsevier, 2 edn., https://doi.org/10.1016/B978-0-12-372522-6.00007-4, http://scholar.google.com/scholar?hl=en&btnG=Search&q=intitle:Nitrogen+Uptake+and+Assimilation#4, 2008.

Osborn, T. R.: Estimates of the local rate of vertical diffusion from dissipation measurements, Journal of Physical Oceanography, 10(1), 83–89, http://journals.ametsoc.org/doi/abs/10.1175/1520-0485(1980)010%3C0083:EOTLRO%3E2.0.CO;2, 1980.

Partensky, F. and Garczarek, L.: Prochlorococcus: advantages and limits of minimalism., Annual review of marine science, 2, 305–31, https://doi.org/10.1146/annurev-marine-120308-081034, http://www.ncbi.nlm.nih.gov/pubmed/21141667, 2010.

Partensky, F., Blanchot, J., and Vaulot, D.: Differential distribution and ecology of Prochlorococcus and Synechococcus in oceanic waters : a review, Bulletin de l'Institut océanographique, 19, 457–475, http://cat.inist.fr/?aModele=afficheN&cpsidt=1218663, 1999a.

Partensky, F., Hess, W., and Vaulot, D.: Prochlorococcus, a marine photosynthetic prokaryote of global significance, Microbiol.Mol Biol.Rev., 63, 106–127, https://doi.org/doi:1092-2172/99/$04.00, http://www.ncbi.nlm.nih.gov/pmc/articles/PMC98958/pdf/mr000106.pdf, 1999b.

Paulsen, M. L., Doré, H., Garczarek, L., Seuthe, L., Müller, O., Sandaa, R.-A., Bratbak, G., and Larsen, A.: Synechococcus in the Atlantic Gateway to the Arctic Ocean, Frontiers in Marine Science, 3, https://doi.org/10.3389/fmars.2016.00191, http://journal.frontiersin.org/article/10.3389/fmars.2016.00191, 2016.

Pinhassi, J., DeLong, E. F., Béjà, O., González, J. M., and Pedrós-Alió, C.: Marine Bacterial and Archaeal Ion-Pumping Rhodopsins: Genetic Diversity, Physiology, and Ecology., Microbiology and molecular biology reviews : MMBR, 80, 929–54, https://doi.org/10.1128/MMBR.00003-16, http://www.ncbi.nlm.nih.gov/pubmed/27630250, 2016.

Prandke, H. and Stips, A.: Test measurements with an operational microstructure-turbulence profiler: Detection limit of dissipation rates, Aquatic Sciences, 60, 191–209, https://doi.org/10.1007/s000270050036, 1998.

R Core Team: R: A Language and Environment for Statistical Computing, http://www.r-project.org/, 2015.

Raven, J. A.: Why are there no picoplanktonic O 2 evolvers with volumes less than 10 - 19 m^3 ?, Journal of Plankton Research, 16, 565–580, https://doi.org/10.1093/plankt/16.5.565, http://plankt.oxfordjournals.org/cgi/doi/10.1093/plankt/16.5.565, 1994.

Raven, J. A.: The twelfth Tansley Lecture. Small is beautiful: The picophytoplankton, https://doi.org/10.1046/j.1365-2435.1998.00233.x, 1998.

Richardson, T. L. and Jackson, G. a.: Small phytoplankton and carbon export from the surface ocean, Science, 315, 838–840, https://doi.org/10.1126/science.1133471, http://www.ncbi.nlm.nih.gov/pubmed/17289995, 2007.

Rusch, D. B., Martiny, A. C., Dupont, C. L., Halpern, A. L., and Venter, J. C.: Characterization of Prochlorococcus clades from iron-depleted oceanic regions., Proceedings of the National Academy of Sciences of the United States of America, 107, 16 184–9, https://doi.org/10.1073/pnas.1009513107, http://www.ncbi.nlm.nih.gov/pubmed/20733077%5Cnhttp://www.pubmedcentral.nih.gov/articlerender.fcgi?artid=PMC2941326, 2010.

Scanlan, D. J. and West, N. J.: Molecular ecology of the marine cyanobacterial genera Prochlorococcus and Synechococcus., FEMS microbiology ecology, 40, 1–12, https://doi.org/10.1111/j.1574-6941.2002.tb00930.x, http://www.ncbi.nlm.nih.gov/pubmed/19709205, 2002.

Schattenhofer, M., Wulf, J., Kostadinov, I., Glöckner, F. O., Zubkov, M. V., and Fuchs, B. M.: Phylogenetic characterisation of picoplanktonic populations with high and low nucleic acid content in the North Atlantic Ocean, Systematic and Applied Microbiology, 34, 470–475, https://doi.org/10.1016/j.syapm.2011.01.008, http://dx.doi.org/10.1016/j.syapm.2011.01.008, 2011.

Sherr, E. B., Sherr, B. F., and Wheeler, P. A.: Distribution of coccoid cyanobacteria and small eukaryotic phytoplankton in the upwelling ecosystem off the Oregon coast during 2001 and 2002, Deep-Sea Research Part II: Topical Studies in Oceanography, 52, 317–330, https://doi.org/10.1016/j.dsr2.2004.09.020, 2005.

Smayda, T. J.: Phytoplankton species succession., Blackwell Scientific Publications, http://ci.nii.ac.jp/naid/10003672033/en/, 1980.

Sommaruga, R., Hofer, J. S., Alonso-Sáez, L., and Gasol, J. M.: Differential sunlight sensitivity of picophytoplankton from surface Mediterranean coastal waters, Applied and Environmental Microbiology, 71, 2154–2157, https://doi.org/10.1128/AEM.71.4.2154-2157.2005, 2005.

Teira, E., Hernando-Morales, V., Fernández, A., Martínez-García, S., Álvarez-Salgado, X. A., Bode, A., and Varela, M.: Local differences in phytoplankton-bacterioplankton coupling in the coastal upwelling off Galicia (NW Spain), Marine Ecology Progress Series, 528, 53–69, https://doi.org/10.3354/meps11228, 2015.

Van Mooy, B., Rocap, G., Fredricks, H. F., Evans, C. T., and Devol, A. H.: Sulfolipids dramatically decrease phosphorus demand by pico-cyanobacteria in oligotrophic marine environments., Proceedings of the National Academy of Sciences of the United States of America, 103, 8607–12, https://doi.org/10.1073/pnas.0600540103, http://www.pnas.org/content/103/23/8607.short, 2006.

Vila-Costa, M., Gasol, J. M., Sharma, S., and Moran, M. A.: Community analysis of high- and low-nucleic acid-containing bacteria in NW Mediterranean coastal waters using 16S rDNA pyrosequencing, Environmental Microbiology, 14, 1390–1402, https://doi.org/10.1111/j.1462-2920.2012.02720.x, 2012.

Villamaña, M., Mouriño-Carballido, B., Cermeño, P., Chouciño, P., da Silva, J., Fernández-Castro, B., Gilcoto, M., Graña, R., Latasa, M., Marañón, E., Otero-Ferrer, J. L., and Scharek, R.: Role of internal waves on mixing, nutrient supply and phytoplankton composition during spring and neap tides in the Ría de Vigo (NW Iberian Peninsula), Limnology and Oceanography, https://doi.org/10.1002/lno.10482, 2017.

Wood, S. N.: Generalized additive models: an introduction with R, CRC press, 2006.

Wood, S. N.: Fast stable restricted maximum likelihood and marginal likelihood estimation of semiparametric generalized linear models, Journal of the Royal Statistical Society. Series B (Methodological), 73, 3–36, 2011.

Wood, S. N., Pya, N., and Säfken, B.: Smoothing Parameter and Model Selection for General Smooth Models, Journal of the American Statistical Association, 111, 1548–1563, https://doi.org/10.1080/01621459.2016.1180986, 2016.

Wooster, W. S., Bakun, A., and McLain, R. M.: Seasonal upwelling cycle along the Eastern boundary of the North Atlantic., Journal of Marine Research, 34, 131–141, 1976.

Worden, A. Z., Nolan, J. K., and Palenik, B.: Assessing the dynamics and ecology of marine picophytoplankton: The importance of the eukaryotic component, Limnology and Oceanography, 49, 168–179, 2004.

Zubkov, M. V., Sleigh, M. A., Burkill, P. H., and Leakey, R. J. G.: Picoplankton community structure on the Atlantic Meridional Transect: A comparison between seasons, Progress in Oceanography, 45, 369–386, https://doi.org/10.1016/S0079-6611(00)00008-2, 2000.
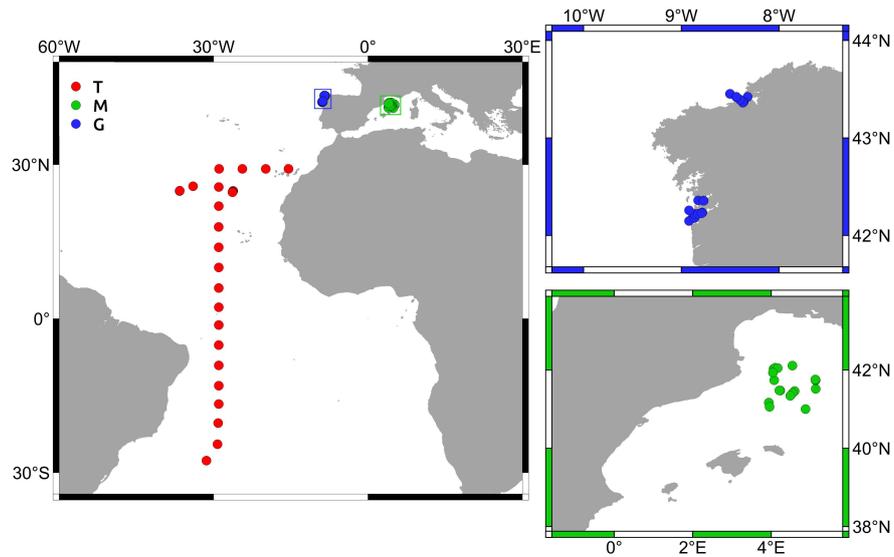
Figure 1. Location of the stations sampled in the tropical and subtropical Atlantic ocean (T), the Mediterranean Sea (M), and the Galician coastal upwelling (G). Small panels provide details about those staions sampled in M (green color) and G (blue color).
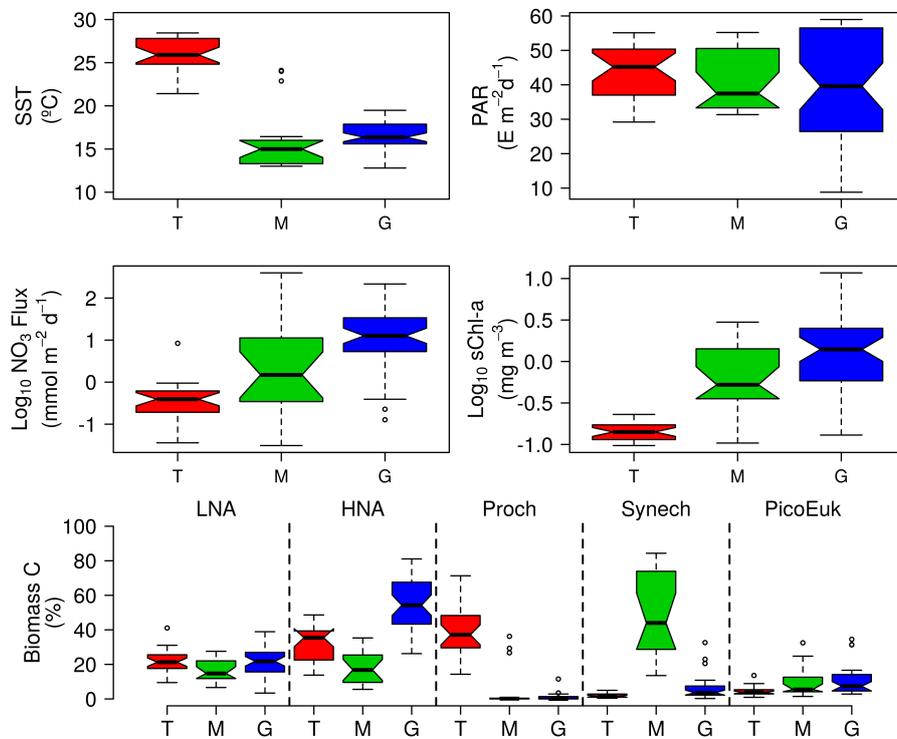
Figure 2. Box-and-whiskers plots of Sea Surface Temperature (SST), surface photosynthetic active radiation (PAR), nitrate supply (NO$_3$ Flux), surface chlorophyll-*a* concentration (sChl-a), and contribution to total picoplankton biomass of low (LNA) and high (HNA) nucleic acid content bacteria, *Prochlorococcus* (Proch), *Synechococcus* (Synech), and small picoeukaryotes (PicoEuk) computed for the tropical and subtropical Atlantic ocean (T), the Mediterranean (M) and the Galician coastal upwelling (G). On each box, the central mark indicates the median, the notches the 95% confidence interval for the median, and the bottom and top edges of the box indicate the 25th and 75th percentiles, respectively. The whiskers extend to the most extreme data points not considered outliers, and the outliers are plotted individually using white circles.
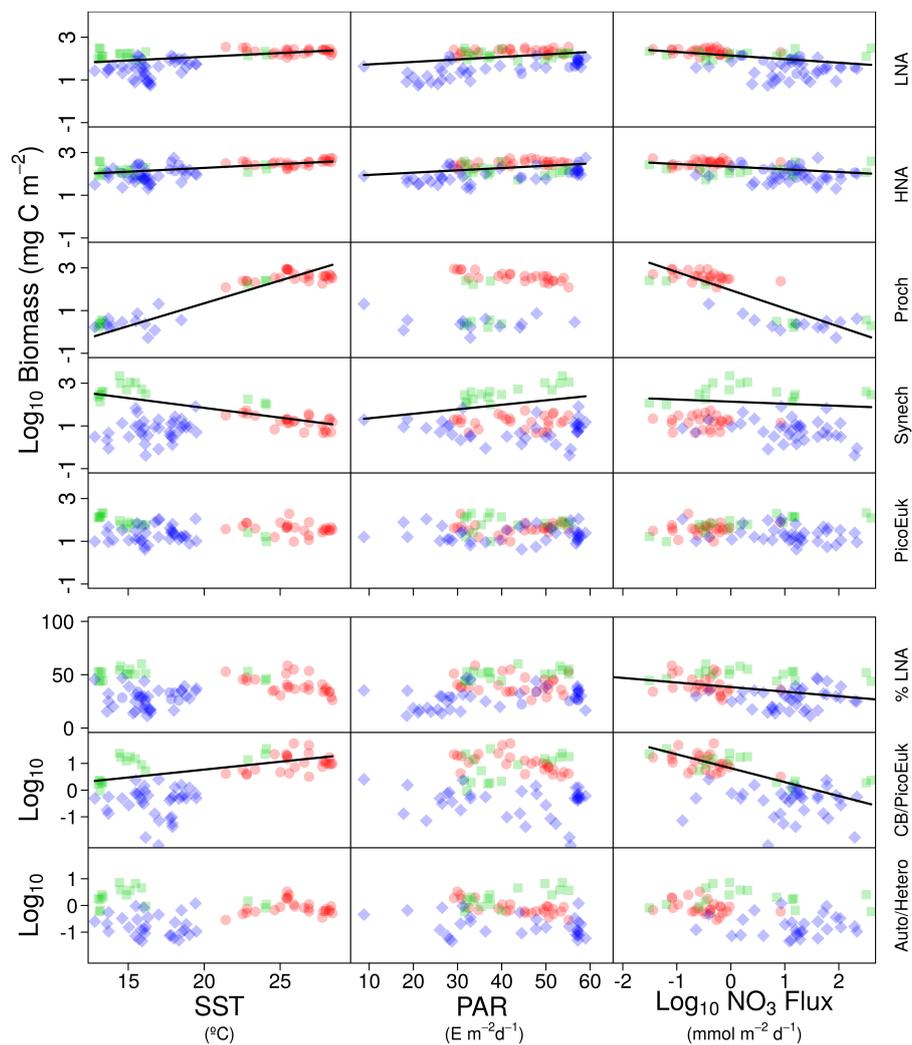
Figure 3. Pair scatter plots representing the relationship between log-transformed depth-integrated biomass for each picoplankton subgroup, the contribution of low nucleic acid content bacteria to heterotrophic picoplankton biomass (%LNA), the ratio of cyanobacteria (*Prochloro-coccus* + *Synechococcus*) to picoeukaryotes depth-integrated biomass (CB/PicoEuK), and the ratio autotrophic to heterotrophic picoplankton biomass (Auto/Hetero) versus sea surface temperature (SST), surface photosynthetically active radiation (PAR) and nitrate flux (NO₃ flux). Significant linear relationships are indicated as solid (p-value < 0.01) black lines. Samples collected at different regions are indicated as red dots (tropical and subtropical Atlantic ocean), green squares (Mediterranean) and blue diamonds (Galician coastal upwelling).
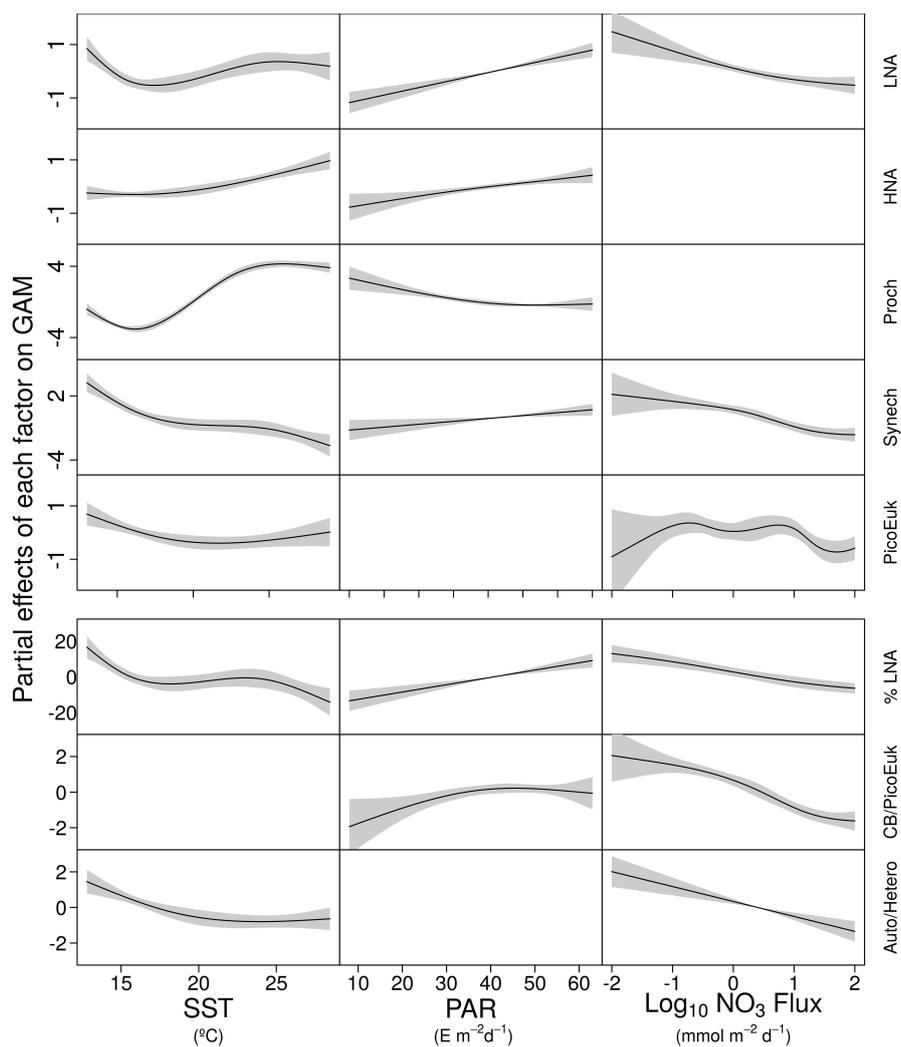
Figure 4. GAM-predicted effects of the response variables (biomass and contribution of picoplankton subgroups) as a smooth function of surface temperature (SST), photosynthetically active radiation (PAR) and nitrate flux (NO₃ flux). All terms were centered in zero. Significant linear relationships are indicated as solid (p-value < 0.01) black lines. Shaded regions represent the 95% confidence intervals of the smooth spline functions. Intercept values were 4.6 (LNA), 5.1 (HNA), 2.1 (*Prochlorococcus*), 3.6 (*Synechococcus*), 3.7 (picoeukaryotes), 36.4 (contribution of LNA to heterotrophic picoplankton, %LNA), 1.4 (cyanobacteria to picoeukaryotes ratio, CB/PicoEuk), and -0.1 (autotrophic to heterotrophic biomass ratio, Auto/Hetero).
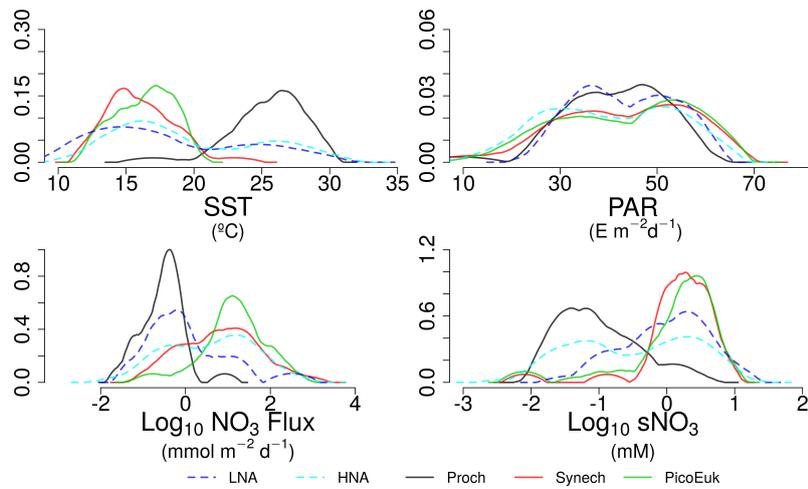
Figure 5. Kernel density estimates of LNA and HNA bacteria, *Prochlorococcus*, *Synechococcus* and picoeukaryotes based on the considered niche descriptors: sea surface temperature (SST), surface photosynthetically active radiation (PAR), nitrate flux (NO_3 flux) and surface concentration (sNO_3).
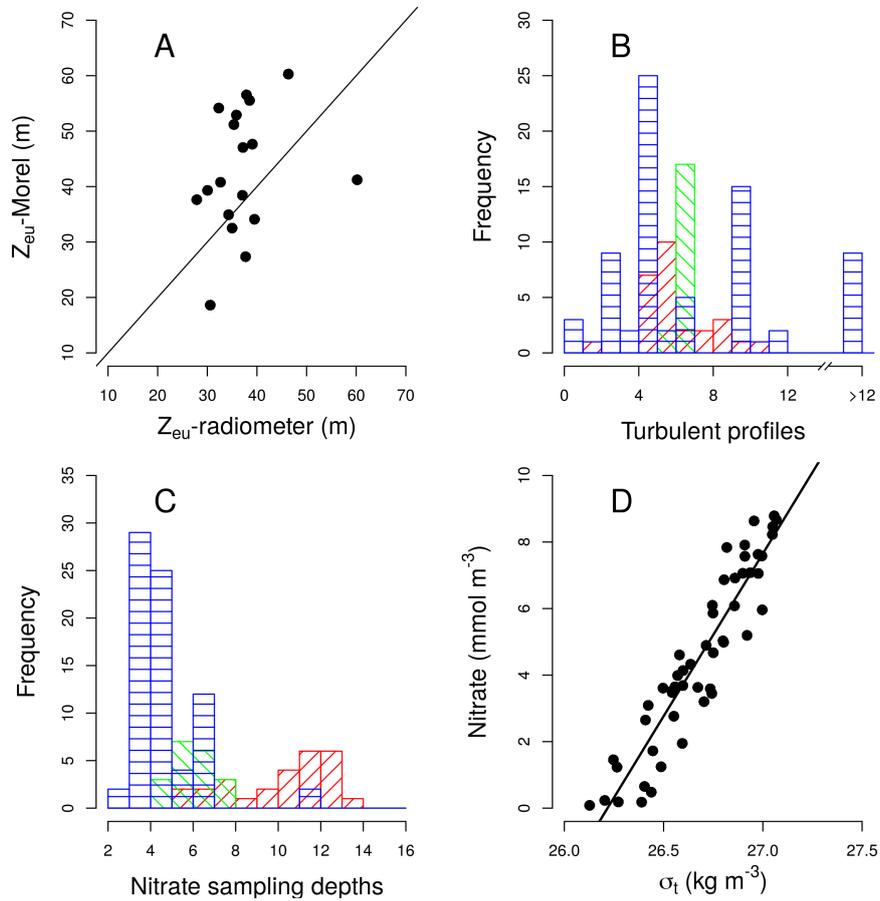
Figure A1. A) Pair scatter plot representing the relationship between the euphotic zone depth (Z_{eu}) computed using the Morel et al. (2007) equation and the data collected by a radiometer during the HERCULES cruises, the solid line represents 1:1 relationship. B) Frequency histogram of the number of turbulence profiles deployed at each station and domain. C) Frequency histograms of the number of samples collected for the determination of nitrate concentration at each station and domain: tropical and subtropical Atlantic ocean (red), the Mediterranean (green) and the Galician coastal upwelling (blue). D) Pair scatter plot representing the relationship between nitrate concentration and density built by using all samples collected during the NICANOR sampling period.
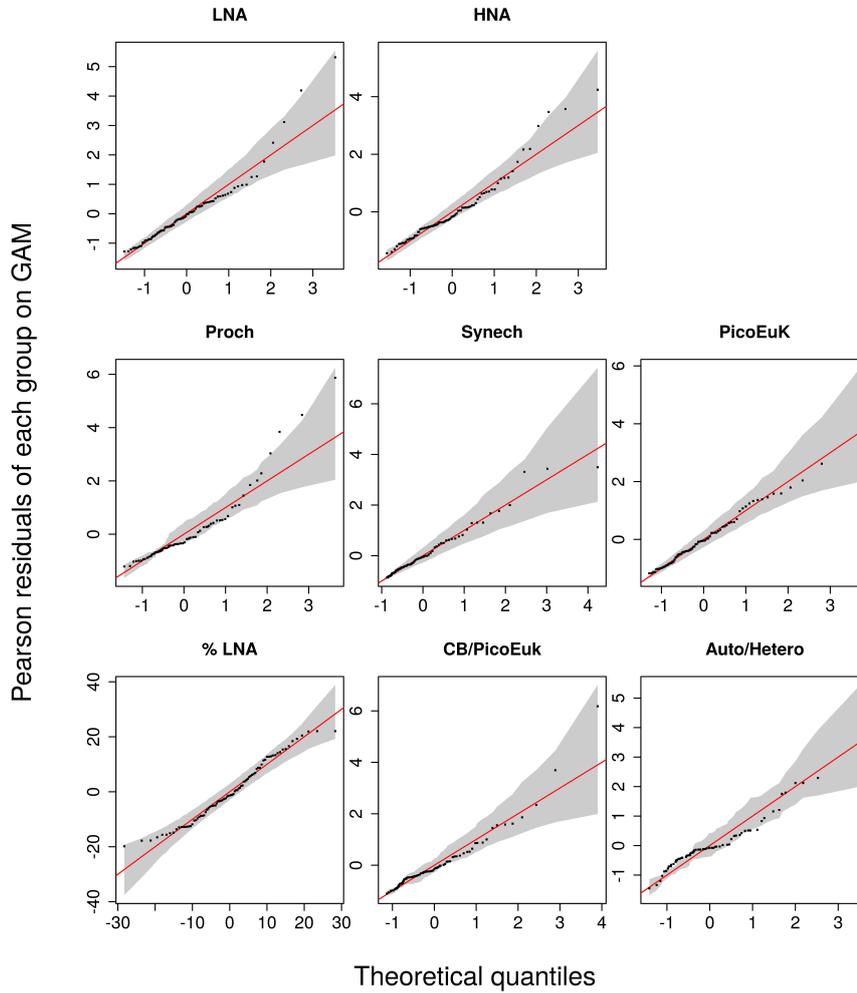
Figure A2. Quantile-Quantile (QQ) plots between the observations and the selected GAM models for each picoplankton subgroup, the contribution of LNA to heterotrophic picoplankton (%LNA), the cyanobacteria to picoeukaryotes ratio (CB/PicoEuk), and the autotrophic to heterotrophic biomass ratio (Auto/Hetero). The y-axes represent the Pearson residuals and the x-axes the negative binomial theoretical quantiles. Solid red lines indicate the theoretical quantile of the models and grey shadows the 95% confidence intervals.
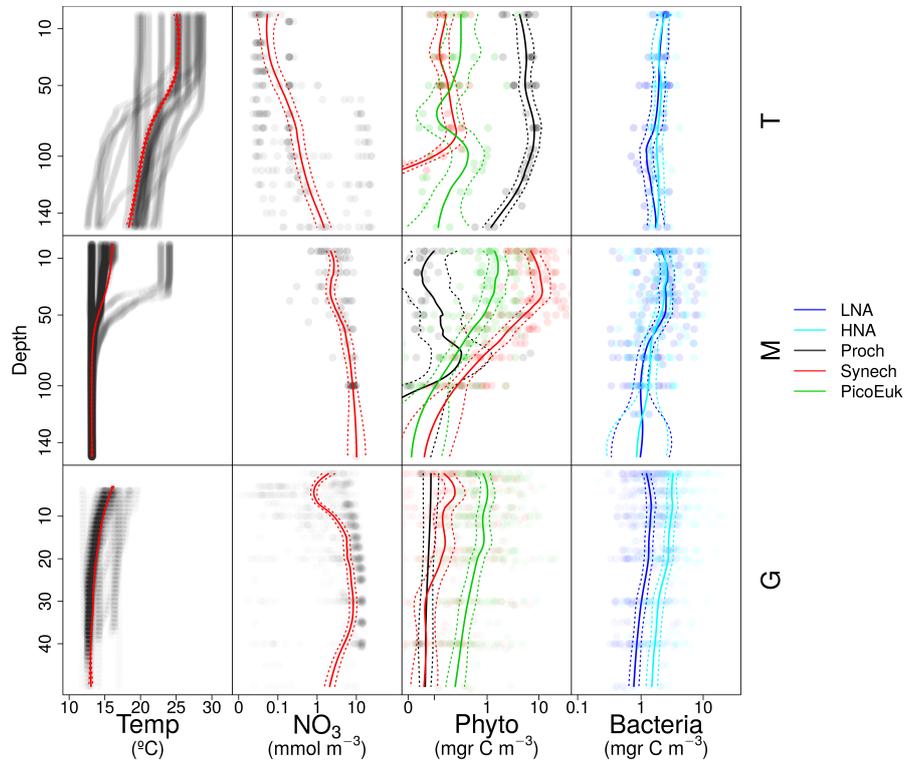
Figure A3. Vertical distribution of temperature (Temp), nitrate (NO₃) and picoplankton biomass of autotrophic (Phyto) and heterotrophic (Bacteria) groups for each domain: tropical and subtropical Atlantic ocean (T), the Mediterranean (M), and the Galician coastal upwelling (G). Points represent raw data and the solid line the locally weighted scatterplot smoothing (LOESS). Dashed lines indicate 95% confidence intervals. Dot and line color intensity indicates the number of overlapping observations.

Table 1. Details of the data included in this study. Domain referred to the tropical and subtropical Atlantic ocean (T), the Mediterranean Sea (M), and the Galician coastal upwelling (G). N indicates the number of stations sampled at each cruise. Duration (mean ± standard deviation, in minutes) is the time used for the turbulence profiler deployment in each station. Depth (mean ± standard deviation, in meters) is the maximum depth reached by the microstructure profiler.

Domain	Region	N	Cruise	Vessel	Date	Duration	Depth
T	NE Atlantic	8	CARPOS	Hespérides	14/10/06- 22/11/06	57 ± 24	137 ± 15
T	Atlantic	18	TRYNITROP	Hespérides	14/04/08 - 02/05/08	45 ± 12	219 ± 19
M	Liguro-Provençal Basin	6	FAMOSO I	Sarmiento de Gamboa	14/3/09 - 22/3/09	66 ± 5	259 ± 38
M	Liguro-Provençal Basin	10	FAMOSO II	Sarmiento de Gamboa	30/4/09 - 13/05/09	94 ± 4	273 ± 2
M	Liguro-Provençal Basin	3	FAMOSO III	Sarmiento de Gamboa	16/09/09 - 20/09/09	133 ± 3	323 ± 24
G	Ría de A Coruña	1	HERCULES I	Lura	07/06/10	20 ± 4	35 ± 2
G	Ría de A Coruña	5	HERCULES II	Lura	28/09/11 - 29/09/11	11 ± 8	33 ± 26
G	Ría de A Coruña	13	HERCULES III	Lura	16/07/12 - 20/07/12	8 ± 5	41 ± 29
G	Ría de Vigo	9	DISTRAL	Mytilus	14/02/12 - 06/11/12	110 ± 76	38 ± 1
G	Ría de Vigo	2	CHAOS	Mytilus	20/08/13 - 27/08/13	1515 ± 6	41 ± 29
G	Ría de A Coruña	12	NICANOR	Lura	27/02/14 - 17/12/15	33 ± 5	62 ± 3
G	Rías de Vigo & Pontevedra	10	ASIMUTH	Ramón Margalef	17/06/13 - 21/06/13	10 ± 4	28 ± 10

Table 2. Mean $\pm$ standard deviation of Sea Surface Temperature (SST), surface Photosynthetic Active Radiation (PAR), Mixed Layer Depth (MLD), Photic Layer Depth (1% PAR), surface nitrate concentration (sNO$_3$), nitrate gradient, vertical diffusivity (K), nitrate supply (NO$_3$ flux), surface chlorophyll (sChl-*a*), photic layer depth-integrated chlorophyll-a (Chl-*a*), biomass (B), abundance (A), and contribution (C) to total picoplankton biomass (Total Pico B), and surface abundance (s) of LNA and HNA bacteria, *Prochlorococcus*, *Synechococcus* and picoeukaryotes computed for the Tropical and subtropical Atlantic ocean (T), the Mediterranean (M), and the Galician coastal upwelling (G). MLD was estimated from an increase in water column density of 0.125 Kg m^{-3} relative to surface values. A nonparametric 1-way ANOVA (Kruskal-Wallis) was performed to test the null hypothesis that independent groups come from same distribution. The Bonferroni multiple comparison test was applied a posteriori to analyze the differences between every pair of groups. $*p < 0.05$; $**p < 0.01$; $***p < 0.001$.

Variables (Units)	T	M	G	KW p-value	Post hoc *Bonferroni*
SST (ºC)	26 ± 2	16 ± 4	16 ± 2	<0.001***	T>G>M
PAR (E m^{-2} d^{-1})	43 ± 23	42 ± 13	39 ± 17	0.69	
MLD (m)	61 ± 30	61 ± 71	12 ± 10	<0.001**	T,M>G
1% PAR (m)	109 ± 23	62 ± 13	37 ± 17	<0.001**	T>M>G
sNO$_3$ (µmol m^{-3})	90 ± 77	2414± 1635	1601 ± 1604	<0.001***	T<M,G
NO$_3$ gradient (µmol m^{-4})	146 ± 158	90 ± 40	105 ± 100	0.71	
K (m^2 s^{-1}) x10^{-3}	0.2 ± 0.3	5.3 ± 13.9	0.5 ± 0.8	0.24	
NO$_3$ flux (mmol m^{-2} d^{-1})	0.7 ± 1.6	41 ± 113	30 ± 46	<0.001***	T<M<G
sChl-*a* (mg m^{-3})	0.1 ± 0.1	0.9 ± 0.9	2.2 ± 2.5	<0.01**	T<M<G
Chl-*a* (mg m^{-2})	31 ± 6	70 ± 99	81 ± 66	<0.001***	T<G
sLNA A (cell ml^{-1}) x105	4.4±2.4	3.7±2.5	2.1±1.1	<0.001***	T>M>G
sHNA A (cell ml^{-1}) x105	3.0±1.8	4.0±4.5	3.6±2.3	0.13	
sProchl A (cell ml^{-1}) x10^3	144±132	2.2±4.4	1.0±2.8	<0.001***	T>M,G
sSynech A (cell ml^{-1}) x10^3	18±66	75±81	5.7±6.9	<0.001***	T<M>G
sPicoEuk A (cell ml^{-1}) x10^3	2.5±9.4	6.8±8.4	5.7±6.9	<0.001***	T<M,G
LNA A (cell m^{-2}) x10^{12}	40 ± 20	22 ± 8	6.4 ± 4	<0.001***	T,M>G
HNA A (cell m^{-2}) x10^{12}	27 ± 1	22 ± 1	9.4 ± 0.8	<0.001***	T>M>G
Prochl A (cell m^{-2}) x10^{11}	156 ± 121	10 ± 23	0.5 ± 1	<0.001***	T>M,G
Synech A (cell m^{-2}) x10^{11}	7 ± 15	50 ± 49	2 ± 2	<0.001***	T<M>G
PicoEuk A (cell m^{-2}) x10^{11}	1.7 ± 3	2.8 ± 2	1 ± 2	<0.001***	T<M>G
LNA B (mg C m^{-2})	253 ± 105	170 ± 97	43 ± 34	<0.001***	T>M>G
HNA B (mg C m^{-2})	216 ± 127	168 ± 105	108 ± 73	0.02*	T>M>G
Prochl B (mg C m^{-2})	482 ± 516	36 ± 84	1.3 ± 4	<0.001***	T>M,G
Synech B (mg C m^{-2})	43 ± 83	576 ± 530	19 ± 26	<0.001***	T,M>G
PicoEuk B (mg C m^{-2})	59 ± 102	86 ± 59	43 ± 59	<0.001***	T<M >G
Total Pico B (mg C m^{-2})	1052 ± 215	1038 ± 485	216 ± 36	<0.001***	T,M>G
LNA C (%)	27 ± 10	18 ± 8	21 ± 9	<0.001***	T>M,G
HNA C (%)	22 ± 12	17 ± 10	55 ± 15	<0.001***	T,M<G
Prochl C (%)	41 ± 16	5 ± 12	1 ± 2	<0.001***	T,M<G
Synech C (%)	4 ± 5	50 ± 24	6 ± 7	<0.001***	T,G>M
PicoEuk C (%)	5 ± 5	10 ± 9	11 ± 9	<0.001***	T<M,G

Table 3. Simple (R^2) and adjusted squared correlation coefficients (Adj-R^2) for simple linear regression and multiple Generalized Additive Models (GAM) built to predict depth-integrated biomass for each picoplankton subgroup, the contribution of LNA bacteria to total heterotrophic picoplankton biomass (% LNA), the ratio cyanobacteria (*Prochlorococcus* + *Synechococcus*) to picoeukaryotes depth-integrated biomass (CB/PicoEuK) and the ratio autotrophic (CB+PicoEuk) to heterotrophic bacteria (LNA + HNA) biomass based on Sea Surface Temperature (SST), surface photosynthetically active radiation (PAR) and nitrate supply (NO_3 flux). Negative binomial distribution was assumed. Multiple model selection was based on stepwise regression and the Akaike Information Criterion (see Methods). Only significant (p-value < 0.05) results are shown. Percentage of total effects represent the contribution of each environmental factor to the variability explained by each GAM model (see methods).

Group	R^2 simple linear			Adj-R^2 multiple regression	Percentage of total effects		
	SST	PAR	NO_3 flux		SST	PAR	NO_3 flux
LNA	0.39	<0.01	0.34	0.55	0.30	0.35	0.35
HNA	0.47	0.05	0.18	0.53	0.52	0.48	
Proch	<0.01		<0.01	0.86	0.72	0.28	
Synech	0.11	<0.01		0.52	0.53	0.16	0.31
PicoEuk				0.23	0.51		0.49
% LNA		0.05	0.12	0.49	0.39	0.26	0.35
CB/PicoEuk	0.25		0.28	0.40		0.38	0.62
Auto/Hetero				0.29	0.39		0.61

Table 4. Partial weighted niche overlap (%) for each environmental factor and picoplankton subgroup. sNO$_3$ represent surface nitrate concentration. Asterisks denote the existence of significant differences between niches (^ $p<0.1$, * $p<0.05$, ** $p<0.01$, *** $p<0.001$).

		LNA	HNA	Proch	Synech	PicoEuk
	LNA	100				
	HNA	85	100			
SST	Proch			100		
	Synech			9***	100	
	PicoEuk			5***	84	100
	LNA	100				
	HNA	80	100			
PAR	Proch			100		
	Synech			80	100	
	PicoEuk			74*	94	100
	LNA	100				
	HNA	69*	100			
NO$_3$ Flux	Proch			100		
	Synech			31***	100	
	PicoEuk			14***	77 ^	100
	LNA	100				
	HNA	73^	100			
sNO$_3$	Proch			100		
	Synech			22***	100	
	PicoEuk			29***	89	100